Global Biogeochemical Cycles®

RESEARCH ARTICLE
10.1029/2023GB007776

Increased Terrestrial Carbon Export and CO_2 Evasion From Global Inland Waters Since the Preindustrial Era

Hanqin Tian[1,2], Yuanzhi Yao[2,3], Ya Li[2,4], Hao Shi[2,4], Shufen Pan[2,5], Raymond G. Najjar[6], Naiqing Pan[1,2], Zihao Bian[2], Philippe Ciais[7], Wei-Jun Cai[8], Minhan Dai[9], Marjorie A. M. Friedrichs[10], Hong-Yi Li[11], Steven Lohrenz[12], and L. Ruby Leung[13]

[1]Schiller Institute for Integrated Science and Society, Department of Earth and Environmental Sciences, Boston College, Chestnut Hill, MA, USA, [2]International Center for Climate and Global Change Research, College of Forestry, Wildlife and Environment, Auburn University, Auburn, AL, USA, [3]School of Geographic Sciences, East China Normal University, Shanghai, China, [4]Research Center for Eco-Environmental Sciences, Chinese Academy of Sciences, Beijing, China, [5]Department of Engineering and Environmental Studies Program, Boston College, Chestnut Hill, MA, USA, [6]Department of Meteorology and Atmospheric Science, The Pennsylvania State University, University Park, PA, USA, [7]IPSL - Laboratoire des Sciences du Climat et de l'Environnement, Centre d'Etudes Orme des Merisiers, Gif sur Yvette, France, [8]School of Marine Science and Policy, University of Delaware, Newark, DE, USA, [9]State Key Laboratory of Marine Environmental Sciences, College of Ocean and Earth Sciences, Xiamen University, Xiamen, China, [10]Virginia Institute of Marine Science, William & Mary, Gloucester Point, VA, USA, [11]Department of Civil and Environmental Engineering, University of Houston, Houston, TX, USA, [12]School for Marine Science and Technology, University of Massachusetts Dartmouth, New Bedford, MA, USA, [13]Atmospheric Sciences and Global Change Division, Pacific Northwest National Laboratory, Richland, WA, USA

Key Points:

- Terrestrial carbon loading since 1800 has increased by 25%, with 23% of this increase exported to the ocean and 59% being emitted to the atmosphere
- Atmospheric CO_2 and N inputs dominated C export increase, while the climate and land use change dominated the decadal variations in CO_2 evasion
- Global inland water recycles and exports nearly half of the net land C sink into the atmosphere and oceans in the 2010s

Supporting Information:

Supporting Information may be found in the online version of this article.

Correspondence to:

H. Tian,
hanqin.tian@bc.edu

Citation:

Tian, H., Yao, Y., Li, Y., Shi, H., Pan, S., Najjar, R. G., et al. (2023). Increased terrestrial carbon export and CO_2 evasion from global inland waters since the preindustrial era. *Global Biogeochemical Cycles*, *37*, e2023GB007776. https://doi.org/10.1029/2023GB007776

Received 22 MAR 2023
Accepted 28 SEP 2023

Abstract Global carbon dioxide (CO_2) evasion from inland waters (rivers, lakes, and reservoirs) and carbon (C) export from land to oceans constitute critical terms in the global C budget. However, the magnitudes, spatiotemporal patterns, and underlying mechanisms of these fluxes are poorly constrained. Here, we used a coupled terrestrial–aquatic model to assess how multiple changes in climate, land use, atmospheric CO_2 concentration, nitrogen (N) deposition, N fertilizer and manure applications have affected global CO_2 evasion and riverine C export along the terrestrial-aquatic continuum. We estimate that terrestrial C loadings, riverine C export, and CO_2 evasion in the preindustrial period (1800s) were 1,820 ± 507 (mean ± standard deviation), 765 ± 132, and 841 ± 190 Tg C yr^{-1}, respectively. During 1800–2019, multifactorial global changes caused an increase of 25% (461 Tg C yr^{-1}) in terrestrial C loadings, reaching 2,281 Tg C yr^{-1} in the 2010s, with 23% (104 Tg C yr^{-1}) of this increase exported to the ocean and 59% (273 Tg C yr^{-1}) being emitted to the atmosphere. Our results showed that global inland water recycles and exports nearly half of the net land C sink into the atmosphere and oceans, highlighting the important role of inland waters in the global C balance, an amount that should be taken into account in future C budgets. Our analysis supports the view that a major feature of the global C cycle–the transfer from land to ocean–has undergone a dramatic change over the last two centuries as a result of human activities.

Plain Language Summary Despite occupying only 1% of the Earth's surface, inland waters (rivers, lakes, and reservoirs) play a critical role in global carbon (C) cycling by linking two of the Earth's largest C pools, terrestrial and marine ecosystems, as well as by exchanging CO_2 with the atmosphere. Inland waters emit and bury C before it reaches the oceans, with important implications for the global C budget. Although global estimates of lateral C fluxes have been made previously, much uncertainty exists in their magnitudes, spatiotemporal patterns, and underlying controls (anthropogenic vs. natural processes). By improving a coupled terrestrial–aquatic model, we assess how climate, land use, atmospheric CO_2, and nitrogen enrichment affected global CO_2 evasion and riverine C export along the terrestrial–aquatic continuum since the 1800s. We estimate a 25% increase in terrestrial C loading since the 1800s, of which 59% was emitted to the atmosphere and 23% was exported to the ocean. The increased riverine C exports were primarily due to increasing atmospheric CO_2 level and nitrogen inputs; additionally, climate and land conversion dominated interannual and decadal variations in CO_2 evasion. Our findings indicate that anthropogenic-induced climate change and multiple environmental stresses since the preindustrial era have resulted in significant increases in terrestrial C export to oceans and CO_2 evasion. Global inland water recycles and exports nearly half of the net land C sink into the atmosphere and ocean, underscoring the importance of inland waters for closing the global carbon budget.

1. Introduction

Inland waters (streams, rivers, lakes, and reservoirs), though occupying only 1% of the Earth surface, represent a vital link connecting two of the largest active carbon (C) pools, terrestrial, and marine ecosystems. Inland waters also serve as an important conduit for the exchange of CO_2 with the atmosphere. Terrestrial C cycle changes can drastically alter the patterns of C loading (C transfer from land to inland waters), which further influences C dynamics in coastal and marine ecosystems (Butman et al., 2016; Cole et al., 2007; Najjar et al., 2018). Through this biogeochemical pathway, inland waters transport, bury and remove C before it reaches coastal oceans, thereby significantly altering the global C budget. Globally, inland waters emit about 2.2 Pg C yr^{-1} (0.7–4.2 Pg C yr^{-1}) to the atmosphere (Lauerwald et al., 2023a; Raymond et al., 2013), offsetting 75% of the contemporary terrestrial CO_2 sink (Friedlingstein et al., 2019, 2022; Le Quéré et al., 2018). However, large uncertainties still exist in the magnitude and variability of C dynamics along the terrestrial–aquatic continuum. In particular, it is not well understood how natural and anthropogenic disturbances have changed terrestrial C loading to inland waters, the burial of C in inland waters, evasion of CO_2 from inland waters, and C delivery to coastal waters over a century-long time scale, with an estimated 2-σ errors in all of these flux changes at the global scale of between 50% and 100% (Regnier et al., 2022).

Inland water C has three main forms: dissolved organic carbon (DOC), dissolved inorganic carbon (DIC), and particulate organic carbon (POC). Each form responds differently to environmental changes. The long-term changes of C exports in dissolved forms (DOC and DIC) have been found to be primarily regulated by air temperature (Laudon et al., 2012; Pastor et al., 2003), while hydrological conditions may explain their short-term variations (Raymond & Oh, 2007). DIC is also influenced by CO_2 evasion, which is also affected by climate and land-use change (Lauerwald et al., 2015). Land conversions can substantially modify the geomorphologic conditions of the land surface, and thus alter soil erosion and the loss of POC (Galy et al., 2015). Additionally, other direct and indirect anthropogenic factors, such as elevated atmospheric CO_2 concentrations, atmospheric nitrogen deposition, and extensive fertilizer application, can cause notable changes in inland water C fluxes (Findlay, 2005; Houghton, 2010).

Previous estimates of inland water C fluxes were mostly derived from statistical relationships between observations and environmental factors (Dai et al., 2012; M. Li et al., 2017; Ludwig et al., 1996) or from bookkeeping methods (Butman et al., 2016). For example, Dai et al. (2012) estimated the magnitude of global riverine DOC export to be 0.21 Pg C yr^{-1} based on observations from 118 rivers around the world. However, these methods are highly dependent on the quality and quantity of field measurements, which limits their use in watersheds with scarce data and high spatio-temporal heterogeneity. Therefore, hybrid models integrating empirical, statistical and mechanistic components, such as the Global Nutrient Export from WaterSheds (Global NEWS) model, have been developed to estimate riverine exports of C and nutrients (Seitzinger et al., 2005) and greenhouse gas emissions from inland waters (Hu et al., 2016; Kroeze et al., 2005; Seitzinger et al., 2000). Nevertheless, the wide use of empirical equations and over-simplified representations of mechanisms for land and aquatic systems in these models can undermine their predictive capability as the performance of empirical equations may substantially decrease under changing environmental conditions (Girardin et al., 2008; Leach & Moore, 2019).

In contrast, process-based modeling is more general and hence more suitable for both hindcasting and forecasting under varied conditions. Though several models have been applied in the estimation of inland water C fluxes in regional and global studies (Hastie et al., 2019), these models are usually run at a coarse spatial resolution that is unable to capture key water transport processes, such as channel routing in headwater zones, which have been shown to be hotspots of greenhouse gas emissions (Battin et al., 2008; Butman & Raymond, 2011; Butman et al., 2016; M. Li et al., 2021; McClain et al., 2003; Raymond et al., 2013). Furthermore, it is difficult for these models to represent the effect of individual land-to-water delivery factors and their interactions within the actual ecosystem (Robertson & Saad, 2013). Yet, such processes largely determine how C cycling in aquatic ecosystems is affected by natural and anthropogenic disturbances. The comparison of the current C models (M. Li et al., 2019; Marescaux et al., 2020; Mayorga et al., 2010; Nakayama, 2022; Nakhavali et al., 2020; Saccardi & Winnick, 2021; H. Zhang et al., 2022) reveals their limited ability to differentiate small stream processes in simulating riverine C dynamics. The representation of C transport across the river-lake-reservoir continuum remains incomplete in these models. Moreover, a subset of these models lacks the inclusion of terrestrial C processes, thereby hampering the overall coupling of terrestrial and aquatic C dynamics.

Here, we describe refinements of the Terrestrial/Aquatic Continuum module of the Dynamic Land Ecosystem Model (DLEM-TAC) that improve representations of coupling of terrestrial and aquatic processes of the C,

nitrogen and water cycles, and their integration across multiple water types (rivers, headwater, lakes and reservoirs) (Tian et al., 2015b; Yao et al., 2021). The process-based, high-resolution DLEM-TAC was used to quantify the magnitude and spatio-temporal patterns of global inland water CO_2 evasion, C burial in aquatic sediments, and the riverine exports of POC, DOC, and DIC from land to oceans during 1800–2019. Moreover, factorial simulations were implemented to attribute changes in global inland water C fluxes to different environmental factors, including climate, land-use change, atmospheric CO_2 concentration, nitrogen deposition, and fertilizer/manure application. Our findings demonstrate the important roles of both climate-related factors as well as human activities in alterations in land-ocean-atmosphere C exchanges.

2. Methods

The DLEM-Terrestrial/Aquatic Continuum (DLEM-TAC) is an integrated modeling framework that encapsulates land and aquatic ecosystem processes (Figure 1). The land component describes terrestrial biophysical characteristics, plant physiological processes, and soil biogeochemistry at a daily time step (Tian et al., 2010); the aquatic component uses C and nutrient loadings as inputs and simulates the biogeochemical dynamics along the land–river–ocean continuum, such as CO_2 evasion, burial, and transport (Yao et al., 2021). Detailed information on the land component can be found in our previous studies (Pan et al., 2021; Tian et al., 2015a). Here, we focus on the improvements in the aquatic component.

2.1. The Routing Scheme of Rivers, Lakes, and Reservoirs

In DLEM-TAC, water transport within the grid cells is separated into three subgrid processes: hillslope routing, subnetwork routing, and main channel routing. A scale-adaptive and physically based model named Model of Scale-Adaptive River Transport (H. Li et al., 2013) was incorporated into DLEM. The water from surface runoff is routed across hillslopes first. The water received by the subnetwork channels from hillslope flow and groundwater discharge flows into the main channel. Note that the subnetwork channels within a 30 arc-min grid cell represent the streams from first to fifth orders (Fekete et al., 2001). The main channel receives water from upstream grid cells and local subnetworks and discharges it to the downstream grid cell. All three sub-grid routing processes use kinematic wave methods (Chow, 1964), which require several physical parameters (channel length, bank-full depth, channel slope, and channel roughness) derived from a 15 arc-second resolution hydrological data set (H.-Y. Li et al., 2015). To represent the floodplain process, the model assumed that, the channel width increases by five times when the water level is higher than the bankfull channel depth. In the scale-adaptive water transport scheme, the length of the subnetwork flow changes with the model grid resolution (H. Li et al., 2013), so the total effective length of small streams (subnetworks) within a grid cell increases with the grid size. Therefore, the parameters of the new water transport module only require minor re-calibration when the model is applied at different resolutions. This way, the scale-adaptive river routing scheme within DLEM allows a simultaneous representation of carbon and nitrogen fluxes on scales from small streams to large rivers within a grid cell (Yao et al., 2020, 2021).

We should note that, dam operations would substantially affect the flow regime, and the associated carbon fluxes of reservoirs behind them as well as their downstream rivers. Here, we further linked lakes and reservoirs with small streams and large rivers in DLEM, forming a stream–river–lake–reservoir corridor (Wollheim et al., 2008). Specifically, lakes with upstream areas smaller than a grid cell are linked to small streams, while those with upstream areas larger than a grid cell are linked to large rivers. The outflow rates of natural lakes were calculated based on the prescribed residence time obtained from Messager et al. (2016). The residence times of reservoirs that linked subnetwork corridor are obtained from the global data databased (Lehner et al., 2011). Reservoirs that are linked to main channels are considered as major reservoirs. The operation rules of major reservoirs were adopted from existing algorithms (Biemans et al., 2011; Haddeland et al., 2006; Hanasaki et al., 2006), which require a reference run with reservoir operation turned off to provide natural water flows as model input.

2.2. Aquatic Carbon Dynamics in DLEM-TAC

The aquatic C module in DLEM-TAC consists of lateral C transport, the decomposition of organic C, the burial of POC, DIC uptake through primary production, and CO_2 evasion (Figure 1a). The dynamics of different C forms within a water body (river, lake, or reservoir) follow the mass balance:

$$\frac{\Delta M_{\mathrm{POC}}}{\Delta t} = F_{a,\mathrm{POC}} - R_{\mathrm{POC}}\, M_{\mathrm{POC}} - v_s\, A_s\, C_{\mathrm{POC}} + P \quad (1)$$

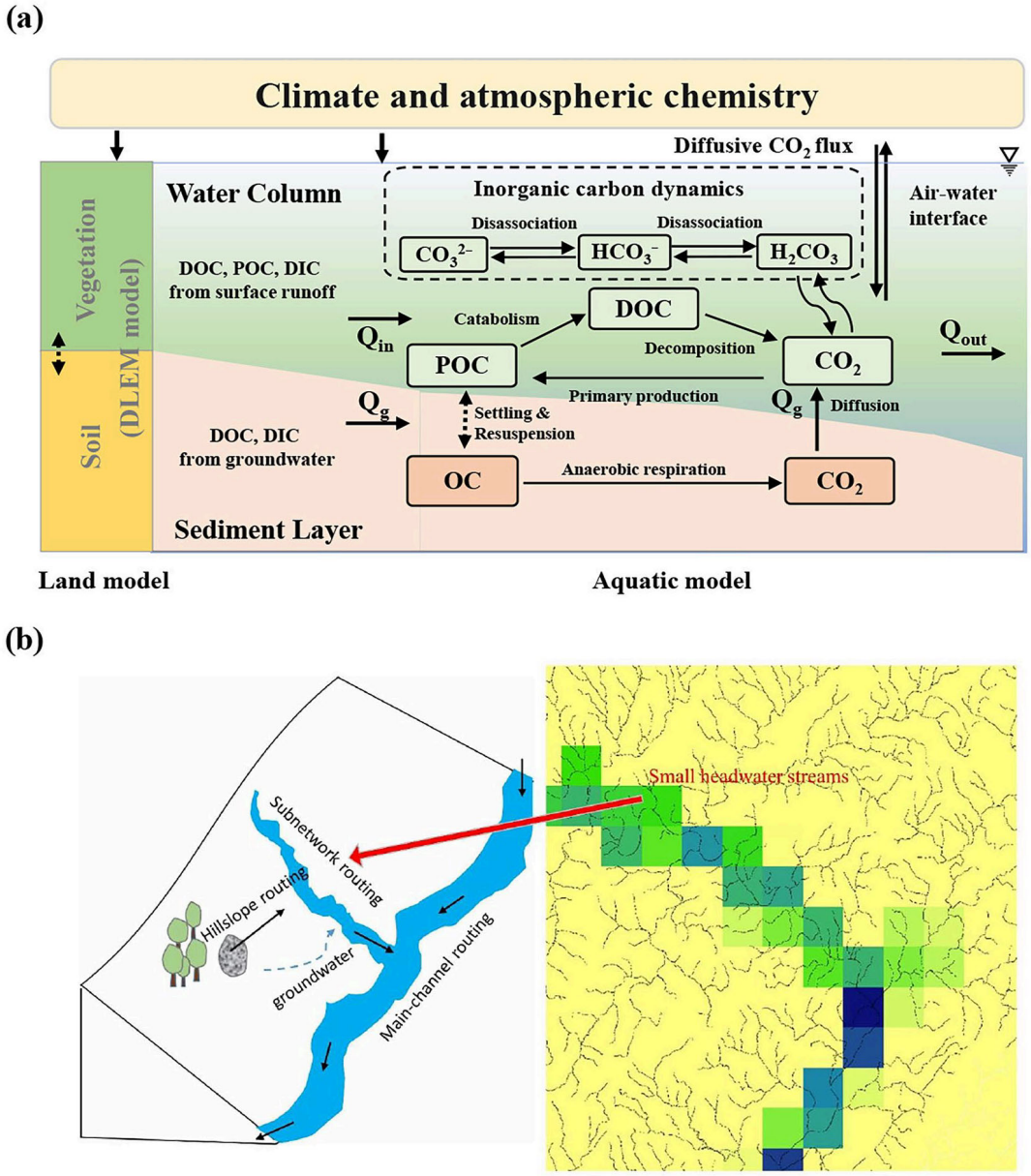

Figure 1. Sources and fates of major carbon species in inland water systems (river, lake, and reservoir) represented in the DLEM-TAC modeling framework (a) and the representation of small rivers within the concept model of the scale-adaptive water transport module (b).

$$\frac{\Delta M_{\mathrm{DOC}}}{\Delta t} = F_{a,\mathrm{DOC}} - R_{\mathrm{DOC}}\, M_{\mathrm{DOC}} + R_{\mathrm{POC}}\, M_{\mathrm{POC}} \tag{2}$$

$$\frac{\Delta M_{\mathrm{DIC}}}{\Delta t} = F_{a,\mathrm{DIC}} - P + R_{\mathrm{DOC}}\, M_{\mathrm{DOC}} - E_{\mathrm{CO_2}} \tag{3}$$

where $\Delta M_{\mathrm{POC}}/\Delta t$, $\Delta M_{\mathrm{DOC}}/\Delta t$, and $\Delta M_{\mathrm{DIC}}/\Delta t$ (g C d^{-1}), are the net changes in the total mass (M) of POC, DOC, and DIC, respectively; Δt denotes the time step (day); F_a represents the net lateral transport (inflow minus outflow) of C species through the linked inland water corridor (g C d^{-1}); R_{DOC} and R_{POC} are the decomposition and catabolism rates of the organic (dissolved and particulate) C species (d^{-1}); v_s is the settling velocity of POC (m d^{-1}); C_{POC} is the concentration of POC (g C m^{-3}); A_s is the area (m^2) of the water body surface, P is the primary production through photosynthesis in the aquatic system (g C d^{-1}), and $E_{\mathrm{CO_2}}$ is the CO_2 evasion to the atmosphere (g C d^{-1}).

Particulate Inorganic Carbon (PIC) was not considered in our simulation because we assumed that PIC is not reactively involved in the C cycle of terrestrial and aquatic ecosystems.

Carbon species (DOC, POC, or DIC) from the land (surface runoff) enter the hillslope and subsurface flows and further contribute to the subnetwork flow (Figure 1b). Biogeochemical processes within the hillslope flow and subsurface flow were not considered in this work. The advective C fluxes through the subnetwork and main-channel are described as

$$F_{a,\mathrm{sub}} = F_{h/c} + F_{g/c} - Q_{\mathrm{sub}} C_{\mathrm{sub}} \tag{4}$$

$$F_{a,\mathrm{main}} = \sum_{\mathrm{i}=0}^{\mathrm{n}} Q_{\mathrm{up},i} C_{\mathrm{up},i} + Q_{\mathrm{sub}} C_{\mathrm{sub}} - Q_{\mathrm{main}} C_{\mathrm{main}} \tag{5}$$

where $F_{a,\mathrm{sub}}$ is the C flux (DOC, POC, or DIC) (g C d^{-1}) of the subnetwork flow; $F_{a,\mathrm{main}}$ is the C flux (g C d^{-1}) of the main-channel flow; $F_{h/c}$ is the C flux (g C d^{-1}) of the hillslope flow; $F_{g/c}$ is the C flux (g C d^{-1}) from the groundwater to the subnetwork; Q_{sub} is the out flow rate of subnetworks (m^3 s^{-1}); C_{sub} is the concentration (g C m^{-3}) of C flux in the subnetworks; Q_{up} and Q_{main} are the outflow rates of upstream grid cells and the main channel within the grid cell (m^3 s^{-1}), respectively; and C_{up} and C_{main} are the associated concentrations (g C m^{-3}) of C species associated with Q_{up} and Q_{main}, respectively.

The first-order decomposition and catabolism rate coefficients are given by

$$R_{\mathrm{DOC}} = K_{\mathrm{DOC}} \left(Q_{10}\right)^{\frac{T_w - T_s}{10}} \tag{6a}$$

$$R_{\mathrm{POC}} = K_{\mathrm{POC}} \left(Q_{10}\right)^{\frac{T_w - T_s}{10}} \tag{6b}$$

where K_{DOC} and K_{POC} are the decomposition and catabolism rates (d^{-1}) at the reference temperature T_s (20°C); Q_{10} is the multiplicative factor applied to the respiration rates when the water temperature T_w (°C) increases by 10°C relative to T_s; and T_w is the water temperature (°C), which is calculated based on an empirical relationship with air temperature (Mohseni et al., 1998, 1999).

The settling velocity of POC is estimated by a simplified Stokes' law (Thomann & Mueller, 1987):

$$v_s = 0.033634\, \alpha \left(\rho_s - \rho_w\right) d^2 \tag{7}$$

where v_s is the settling velocity (m d^{-1}); α represents the effect of the particle shape on the settling velocity; ρ_s and ρ_w are the densities of the particle and water (g · cm^{-3}), respectively; and d is the particle diameter (μm).

The CO_2 exchange between water bodies and the atmosphere is explicitly estimated as

$$E_{\mathrm{CO_2}} = K_{\mathrm{CO_2}} \cdot \left(C_{\mathrm{CO_2}} - C_{\mathrm{CO_2eq}}\right) \cdot A_s \tag{8}$$

where $E_{\mathrm{CO_2}}$ is a net CO_2 evasion (g C d^{-1}); $K_{\mathrm{CO_2}}$ is the gas transfer velocity (m d^{-1}), which is obtained from Raymond et al. (2012); $C_{\mathrm{CO_2}}$ is the dissolved CO_2 concentration (g C m^{-3}), which is computed from DIC and pH (note that pH is a static map interpolated based on the GLORICH data set without temporal variations) at a given water temperature T_w (Hartmann et al., 2019; Yao et al., 2021), and $C_{\mathrm{CO_2eq}}$ is the equilibrium surface water CO_2 concentration (g C m^{-3}) with respect to atmospheric pCO_2.

The gas exchange rate (or refers to piston velocity) $K_{\mathrm{CO_2}}$ (m d^{-1}) is estimated as:

$$K_{\mathrm{CO_2}} = K_{600} \times \left(\frac{\mathrm{SC_{CO_2}}}{600}\right)^{0.5} \tag{9}$$

where $\mathrm{SC_{CO_2}}$ is the Schmidt Number for CO_2 (unitless), which can be calculated as (Raymond et al., 2012):

$$\mathrm{SC_{CO_2}} = 1911 - 118.11 \times T_w + 3.453 \times {T_w}^2 - 0.0413 \times {T_w}^3 \tag{10}$$

where K_{600} (m d^{-1}) is the gas exchange coefficient.

The K_{600} for streams and rivers was estimated by Raymond et al. (2012):

$$K_{600} = \mathrm{VS} \times 2814 + 2.02 \quad (11)$$

In the updated version of DLEM-TAC (Yao et al., 2022), we used different K_{600} for lakes and reservoirs, which was adopted from the work of Tan et al. (2015):

$$K_{600} = 2.778 \cdot 10^{-6} \times \left(2.07 + 0.125 \cdot {U_{10}}^{1.7}\right) \quad (12)$$

where U_{10} is the wind speed of 10-m above the ground surface (m s^{-1}). More detailed information about the representation of the aquatic C dynamics can be found in our previous publication (e.g., Tian et al., 2015a; Yao et al., 2021, 2022).

3. Model Input Data and Simulation Protocol

3.1. Model Forcing

A database at a spatial resolution of 0.5°, consisting of climate variables, land-use change, nitrogen deposition, nitrogen fertilizer, and manure application (Figure S1 in Supporting Information S1), atmospheric CO_2 concentration, and hydrological data was developed to drive the DLEM-TAC model.

The climate variables, which consist of daily precipitation, daily mean temperature, daily maximum temperature, daily minimum temperature, daily wind speed and daily shortwave radiation, were compiled from the CRU–NCEP data set for 1901–2019 (Viovy, 2018). Climate data of each year during 1800–1900 were randomly sampled from the years between 1901 and 1920. The land use data were from HYDE version 3.2 (Klein Goldewijk et al., 2017), and the land cover cohort within a grid cell is composed of four natural vegetation types, one cropland type, and other non-vegetation land-use types (Tian et al., 2018). Detailed information on DLEM land-use input data can be found in M. Liu and Tian (2010).

The annual atmospheric CO_2 concentration from 1800 to 2019 was obtained from the NOAA GLOBALVIEW-CO_2 data set (https://www.esrl.noaa.gov). The nitrogen deposition data set was obtained from the Atmospheric Chemistry and Climate Model Intercomparison Project. The N fertilizer data were obtained from Lu and Tian (2017) and the spatial manure N application data were adopted from B. Zhang et al. (2017) (Figure S2 in Supporting Information S1).

The hydrological input data, covering the flow direction, flow distance, and upstream area, were obtained from the Dominant River Tracing (DRT) data set (Wu et al., 2012). The bank-full width and bank-full depth data sets were obtained from the Hydrological Modeling and Analysis Platform (Getirana et al., 2012). The channel density and channel slopes of small streams and rivers were derived from the National Hydrography Dataset plus v2 data (available at: http://www.horizon-systems.com/NHDPlus/index.php). Surface area, upstream area, volume, depth, and averaged residence time for lakes were obtained from the Hydrolakes data set (Messager et al., 2016). The variables for reservoirs, including built year, height, maximum storage, water surface area, residence time, and upstream area, were obtained from the GRanD database (Lehner et al., 2011).

3.2. Simulation Protocol

DLEM-TAC simulation covered the globe primarily following three steps (Figure 2): (a) To obtain the initial climatological or steady state pre-industrial conditions, we conducted the equilibrium simulation for each grid cell by holding all the driving forces constant in the year 1800 including climate status (we used 1901 climate because CRU–NCEP data before 1901 are not available), land-use conversions, atmospheric CO_2 concentration, and nitrogen additions. When the local C, nitrogen, and water pools of all the grid cells reached a steady state, the equilibrium run finished (Thornton & Rosenbloom, 2005). (b) Before moving to the year-to-year normal simulation, we conducted a 30-year second spin-up run by randomly selecting climate forcings within the 1800s (Tian et al., 2012). Then we conduct the natural flow simulation with the dam module temporarily disabled, and all the driving variables changing over time. (c) After the natural flow simulation, we set up a management flow simulation, with the dam module turned on. We evaluated the simulated flow discharge and C fluxes with

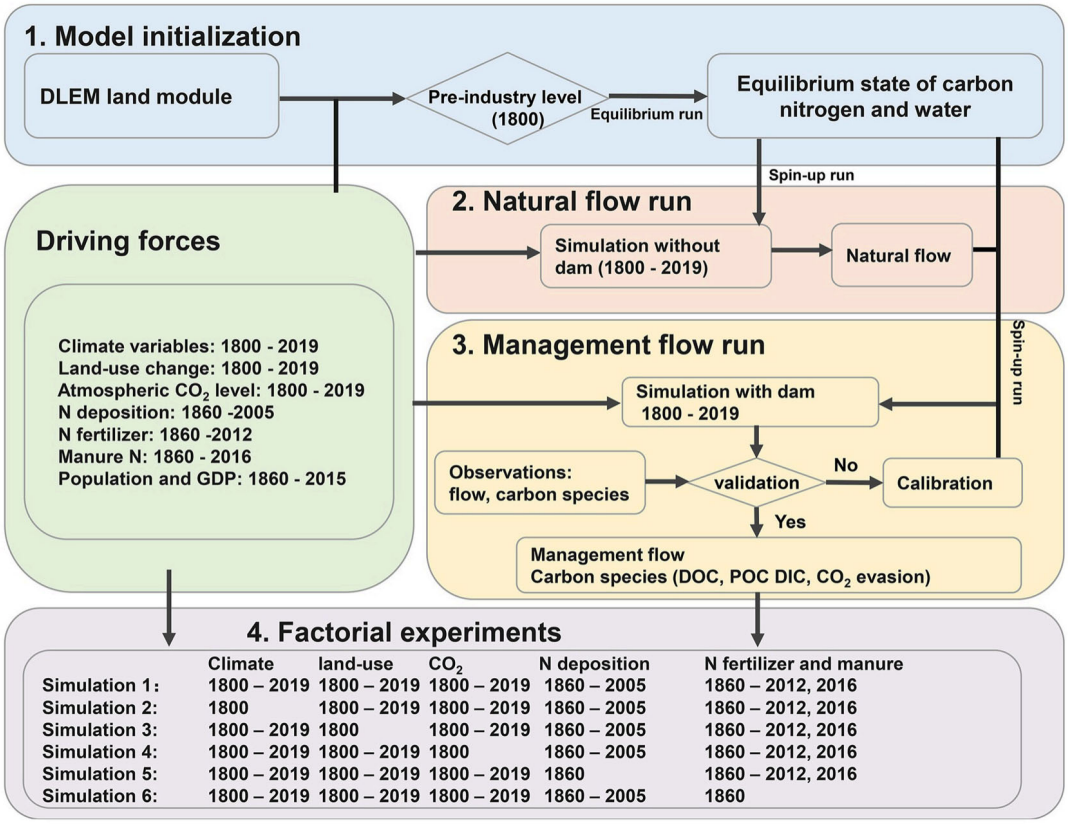

Figure 2. The flowchart representing the simulation protocol for the lateral carbon fluxes.

observations and calibrated the model parameters, including terrestrial C loadings and aquatic processes. Following the model calibration, we conducted the base simulation (S1) by changing all the driving forcing over time to investigate the spatial and temporal patterns of inland water C fluxes.

In order to investigate the responses of inland water C fluxes to multiple environmental changes, six factorial experiments were conducted by fixing each of the driving forcings (Figure 2). For each of the simulations S2 through S6, we held climate, land use, atmospheric CO_2 concentration, nitrogen deposition, fertilizer applications, and manure applications constant at the level of 1800, respectively, while allowing the other variables to track their historical trajectories. The effects of climate, land use, atmospheric CO_2 concentration, nitrogen deposition, fertilizer applications, and manure applications on C loading were calculated by subtracting the factorial experiment from the base simulation (i.e., S1–S2, S1–S3, S1–S4, S1–S5, and S1–S6, respectively).

3.3. Model Evaluation

To examine the performance of DLEM-TAC, we compared the simulated terrestrial loading and riverine export with observations for each C species (at 56 land sites and 47 world major rivers. The detailed data used for model calibration and validation are shown in Figure S3, Tables S1 and S2 in Supporting Information S1). The determination coefficient (R^2) and Nash-Sutcliffe efficiencies (NSE, Nash and Sutcliffe (1970)) were applied to assess the performance of DLEM-TAC. The NSE ranges between $-\infty$ and 1. An NSE close to 1 means a good match of the simulated to the observed data; NSE = 0 means that the simulation is as skillful as the average of the observed data (M. Li et al., 2019). Simulated terrestrial loading of DOC, POC, and DIC agreed well with observations (log transformed, $R^2 > 0.7$; Figure 3a–3c). Aquatic module simulations of the observed annual mean discharges and the C export to the coast were consistent with those recorded by the GEMS-GLORI database (Meybeck & Ragu, 2012), with R^2 values of the log of discharge and export of DOC, POC, and DIC being 0.8, 0.8, 0.6, and 0.7, respectively (Figures 3d–3g), which can be considered as satisfactory (Moriasi et al., 2015). Furthermore, the simulated monthly riverine C exports of the major rivers by

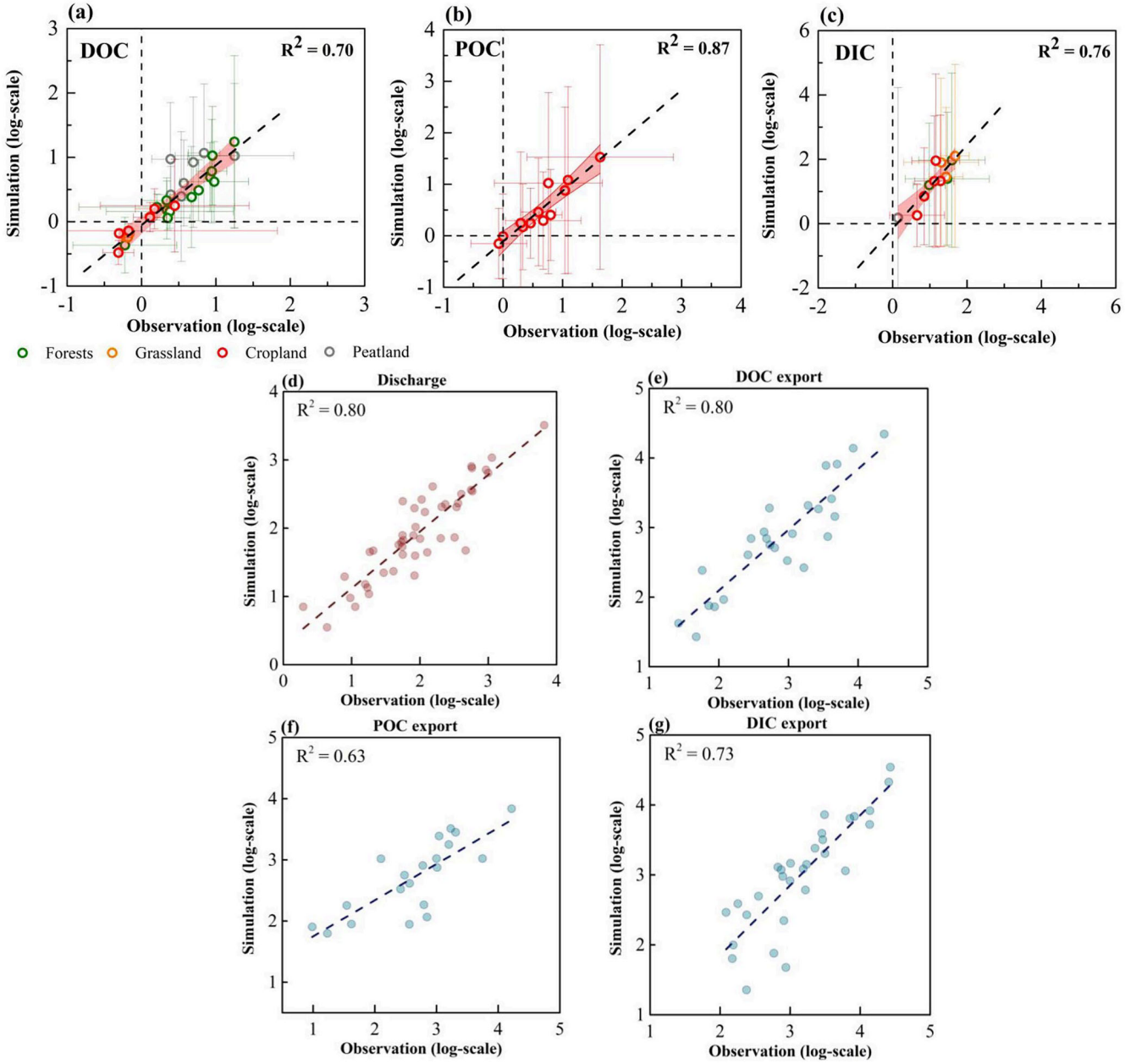

Figure 3. (a–c) Comparisons of simulated carbon loading, (d) river discharge, and (e–g) carbon export with observations. The original units of the carbon loadings, discharge, and carbon exports were g C m^{-2} yr^{-1}, 10^9 m^3 yr^{-1}, and Gg C yr^{-1}, respectively. All data are plotted in log10 scale. In the subplots (a–c)c, the error bars of the observations represent the standard deviation; the error bars of the simulation represent the standard deviation of the simulation from 1981 to 2015. The sources of observed data used to validate carbon loading and carbon exports are provided in Tables S1 and S2 in Supporting Information S1. The red bands in subplot (a–c) represents the 95% confidence bands.

DLEM-TAC performed well in representing the seasonal variability (Figure S4 in Supporting Information S1). We evaluated the simulated performance of seasonal variability on DOC exports at 10 sites, with 3 rivers located in the tropical region, 5 rivers in the temperate region, and 2 rivers in the boreal region. Comparisons between simulated and database observations had R^2 higher than 0.5 and NSEs higher than zero at most sites. We did not evaluate monthly POC exports due to lack of data availability. Additionally, simulated total organic carbon exports of 5 temperate rivers and 3 boreal rivers were comparable to observed values with R^2 values in most cases higher than 0.4 and NSEs higher than zero. Finally, the DIC exports simulated by DLEM-TAC in 3 tropical rivers and 9 temperate rivers were representative of observations with R^2 values higher than 0.5 and higher than zero at most sites.

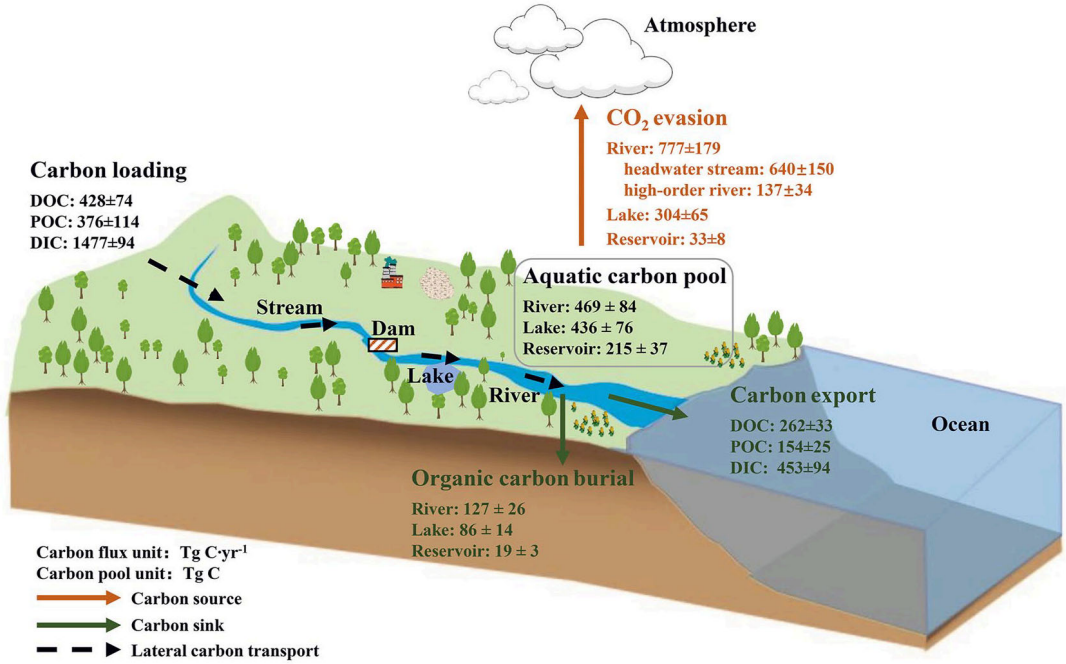

Figure 4. The global inland water carbon budget in the 2010s. Note that carbon burial in rivers includes processes within bankfull channels and floodplains.

3.4. Uncertainty Analysis

We evaluated two major sources of uncertainty in estimating global inland water C fluxes, namely terrestrial C loading and water surface area. To evaluate the uncertainty induced by the former, we carried out a literature survey to collect the observed C loading at the site level. We conducted linear regressions to evaluate the model estimated C loadings against the observations (Figure 3). The 95% confidence band of the linear regressions of DOC, POC, and DIC loadings vary about ±20%, ±30%, and ±40%, respectively, with respect to the 1:1 line. We then conducted two model simulations from 1800 to 2019 with the parameters of terrestrial loadings for DOC, POC, and DIC varying ±20%, ±30%, and ±40%, respectively, to represent their minimal and maximal range. For water surface area, we did not investigate the uncertainty originating from the areas of lake and reservoirs and large rivers, because they can be measured using remotely sensed products, leaving the area of headwater streams as the most uncertain one. We therefore implemented an uncertainty analysis for the river shape parameter (*r* *in* Text S3 in Supporting Information S1) to represent the global river surface areas varying from 0.89, 0.81, 0.73, 0.65, and 0.56 (10^6 km^2), which aligns well with previous estimates (Allen & Pavelsky, 2018; Bastviken et al., 2011; Raymond et al., 2013). We averaged the simulated mean values for two sources of uncertainties and the best-performing simulation, is presented as the final results in this study. The combined standard deviation was calculated as the square root of the sum of the squared individual standard deviations corresponding to each uncertainty source.

4. Results

4.1. The Contemporary Carbon Budget of Global Inland Water Systems

The simulated total terrestrial C loading during 2010–2019 was estimated to be 2281 ± 640 Tg C yr^{-1} (mean ± 1 standard deviation of the annual average, $n = 20$, Figure 4), with DIC dominating, followed by DOC and POC. More than one third (38%) of the C loading (869 ± 151 Tg C yr^{-1}) was exported to the coastal area, of which DIC accounted for half with DOC and POC occupying a similar share. CO_2 evasion was 1,113 ± 251 Tg C yr^{-1}, mainly contributed from rivers (777 ± 179 Tg C yr^{-1}, of which 640 ± 150 Tg C yr^{-1} from headwater streams and 137 ± 34 Tg C yr^{-1} from high-order rivers). The C buried in inland waters was 232 ± 41 Tg C yr^{-1}, much smaller than C export and CO_2 evasion.

Table 1
Global Carbon Fluxes Along the Land-Aquatic Interface (Tg C yr^{-1}, Uncertainty Ranges With Mean ± std)

Carbon species	1800s	1860s	1920s	1980s	2010s
Terrestrial carbon loadings					
DOC	381 ± 66	383 ± 67	391 ± 68	425 ± 73	428 ± 74
POC	232 ± 71	232 ± 71	258 ± 79	294 ± 90	376 ± 114
DIC	1,207 ± 82	1,248 ± 83	1,325 ± 88	1,441 ± 89	1,477 ± 94
Total	1,820 ± 507	1,863 ± 517	1,974 ± 544	2159 ± 598	2281 ± 640
Riverine carbon exports					
DOC	246 ± 31	246 ± 31	255 ± 32	256 ± 32	262 ± 33
POC	114 ± 20	114 ± 20	127 ± 22	137 ± 22	154 ± 25
DIC	405 ± 82	412 ± 83	437 ± 88	439 ± 89	453 ± 94
Total	765 ± 132	773 ± 133	818 ± 141	832 ± 143	869 ± 151
Inland water CO_2 Evasion					
Rivers	595 ± 138	617 ± 142	660 ± 150	750 ± 171	777 ± 179
Headwater streams	481 ± 114	501 ± 118	540 ± 125	619 ± 144	640 ± 150
High-order rivers	114 ± 28	116 ± 28	120 ± 29	131 ± 32	137 ± 34
Lakes	245 ± 53	256 ± 54	268 ± 56	297 ± 62	304 ± 65
Reservoirs	0.0	0.8 ± 0.2	2 ± 1	27 ± 6	33 ± 8
Total	841 ± 190	874 ± 196	931 ± 205	1,074 ± 238	1,113 ± 251

4.2. Long-Term Trend in Inland Water Carbon Fluxes Since the 1800s

In the 1800s, the terrestrial C loading was estimated to be 1,820 ± 507 Tg C yr^{-1}, and more than half of the loading was composed of DIC (1,207 ± 82 Tg C yr^{-1}). An estimated 42% of the C loading was exported from rivers to the ocean (765 ± 132 Tg C yr^{-1}), of which DIC accounted for the largest proportion (404 ± 82 Tg C yr^{-1}), followed by DOC (246 ± 31 Tg C yr^{-1}) and POC (114 ± 20 Tg C yr^{-1}). Nearly half of the C loading leaving inland waters was through CO_2 evasion (841 ± 190 Tg C yr^{-1}) (Table 1).

Model simulations of terrestrial C loading increased gradually from the 1800s (1,820 ± 507 Tg C yr^{-1}) to the 2010s (2281 ± 640 Tg C yr^{-1}), at an average rate of 2 Tg C yr^{-1}. Compared with the 1800s, the total terrestrial C loading in the 2010s increased by 25%, with the loadings of DIC, DOC, and POC increasing by 22%, 12%, and 62%, respectively (Table 1). Enhanced terrestrial C loading resulted in an increase of 31% in the inland water CO_2 evasion compared with the pre-industrial level, predominantly from headwater streams (Table 1). In addition, due to climate change and human activities, CO_2 evasion from inland waters increased significantly after the 1950s, at a rapid rate of 2 Tg C yr^{-1} (Figures 4 and 5). As a result, the fractional increase in riverine C export (14%) from the 1800s to the 2010s was smaller than the corresponding increase in C loading (Figure 5).

4.3. Spatio-Temporal Patterns of Inland Water Carbon Fluxes

At the global scale, tropical regions and the middle and high latitudes of the Northern Hemisphere were the hot spots of the terrestrial C loading. From the pre-industrial period to the recent decade, the terrestrial DOC loading increased in regions of the tropics and high latitudes, such as the Amazon basin, southeastern Asia, and Europe (Figures 6a–6d). Similarly, POC loading increased in the tropics and the regions around 30–45°N (Figures 6e–6h). At the same time, a small part of the Amazon basin was characterized by a decrease in POC loading. In contrast to organic C loading, the largest increase in DIC loading occurred in regions between 30°N and 60°N, such as eastern North America and Europe (Figures 6i–6l).

Consistent with the pattern of C loading, the hot spots of riverine CO_2 evasion were primarily located in the middle and high latitudes of the Northern Hemisphere and in the tropics (Figures 7a–7d). Compared with the pre-industrial period, the contemporary CO_2 evasion from streams and rivers increased notably around the Equator and in the temperate regions of the Northern Hemisphere (30°N–60°N). Due to the abundance of lakes,

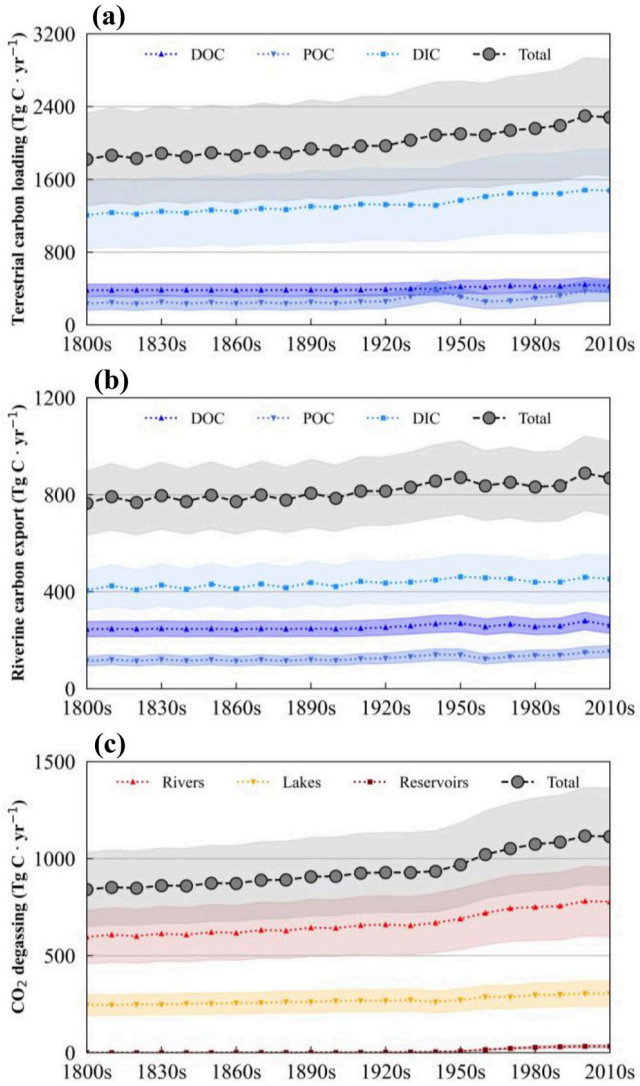

Figure 5. The long-term trajectories of decadal averages of (a) terrestrial carbon loading, (b) riverine exports, and (c) inland water CO_2 evasion from the 1800s to the 2010s. Note that the vertical scales of the subplots are different. The shaded areas represent decadal variations with ±1 standard deviation.

the regions around 50°N contributed most of the lacustrine CO_2 evasion. Since the magnitude of riverine C loading was much larger than that of lakes and reservoirs, the total CO_2 evasion from inland waters was dominated by streams and rivers (Figures 7i–7l).

We analyzed the global inland water C fluxes in the 10 main regions defined by the REgional Carbon Cycle Assessment and Processes Phase 2 project (Ciais et al., 2022). In the recent decade, the largest riverine C exports were from South America, Southeast Asia, North America, and Africa, which accounted for 27%, 17%, 11%, and 11% of the global riverine C exports, respectively (Figure 8). Large increases in C exports were found in North America, Southeast Asia, East Asia, and Russia, accounting for 21%, 15%, 17%, and 18% of the increase in global riverine C exports, respectively. Regions of North America, Europe, Russia, South America and East Asia contributed to most of the CO_2 evasion from global inland waters (23%, 18%, 17%, 12%, and 8%, respectively), and experienced large increases in CO_2 evasion since the pre-industrial period (20%, 27%, 27%, 9%, and 5% of the increase in global CO_2 evasion, respectively) (Figure 8).

4.4. Environmental Controls Over Inland Water Carbon Fluxes

We quantified the contributions of key environmental drivers to the changes in inland water C fluxes through multiple factorial simulation experiments as described in Figure 3. The results showed that, from the pre-industrial period to the recent decade, increases in atmospheric CO_2 concentration caused increases of 17, 15, and 13 Tg C yr^{-1} in the exports of DOC, POC, and DIC, respectively (Figure S6 in Supporting Information S1). Nitrogen additions from fertilizer and manure application and nitrogen deposition were associated with increased exports of DOC, POC, and DIC export by 18, 23, and 25 Tg C yr^{-1}, respectively, over the same time period (Figure S6 in Supporting Information S1). Climate changes primarily influences the exports of DIC (22 Tg C yr^{-1}), followed by the exports of DOC (12 Tg C yr^{-1}) and POC (7 Tg C yr^{-1}) (Figure S6 in Supporting Information S1). Land-use change resulted in an increase in POC exports and DIC exports by 20 and 27 Tg C yr^{-1} in the 2010s, but reduced DOC exports by 2 Tg C yr^{-1} (Figure S6 in Supporting Information S1). Changes in climate and land-use were the dominant factors that increased the CO_2 evasion, by about 88 and 108 Tg C yr^{-1}, respectively, from the 1800s to the 2010s, while other factors (elevated atmospheric CO_2, nitrogen deposition, and fertilizer and manure application) contributed 81 Tg C yr^{-1} (Figure 9). Terrestrial C loadings have similar response patterns to environmental change as riverine C exports (Figure 9). Changes in Climate and land use were the primary factors contributing to changes in terrestrial DOC and DIC loadings during the 1800s–2010s, respectively (Figure S7 in Supporting Information S1). The impact of climate change on terrestrial POC loadings was predominant before the 1950s, while anthropogenic disturbances became more influential than climate change in increasing POC loading after that period (Figure S7 in Supporting Information S1).

The spatial pattern of the dominant factors affecting terrestrial C loading and inland water CO_2 evasion also changed from the early 19th century (1800–1819) to the early 21st century (2000–2019) (Figure 10). In the early 19th century, climate variables were largely responsible for the change in C loading and CO_2 evasion. In comparison, the changes in small parts of Europe, South Asia, coastal regions in East Asia, and southeastern regions in North America were dominated by land use (Figures 10a and 10c). As compared to the early 19th century, the area dominated by land use and nitrogen addition significantly expanded in the early 21st century. Increasing atmospheric CO_2 concentration has become an important factor dominating changes in C loading and CO_2 evasion in Africa (Figures 10b and 10d).

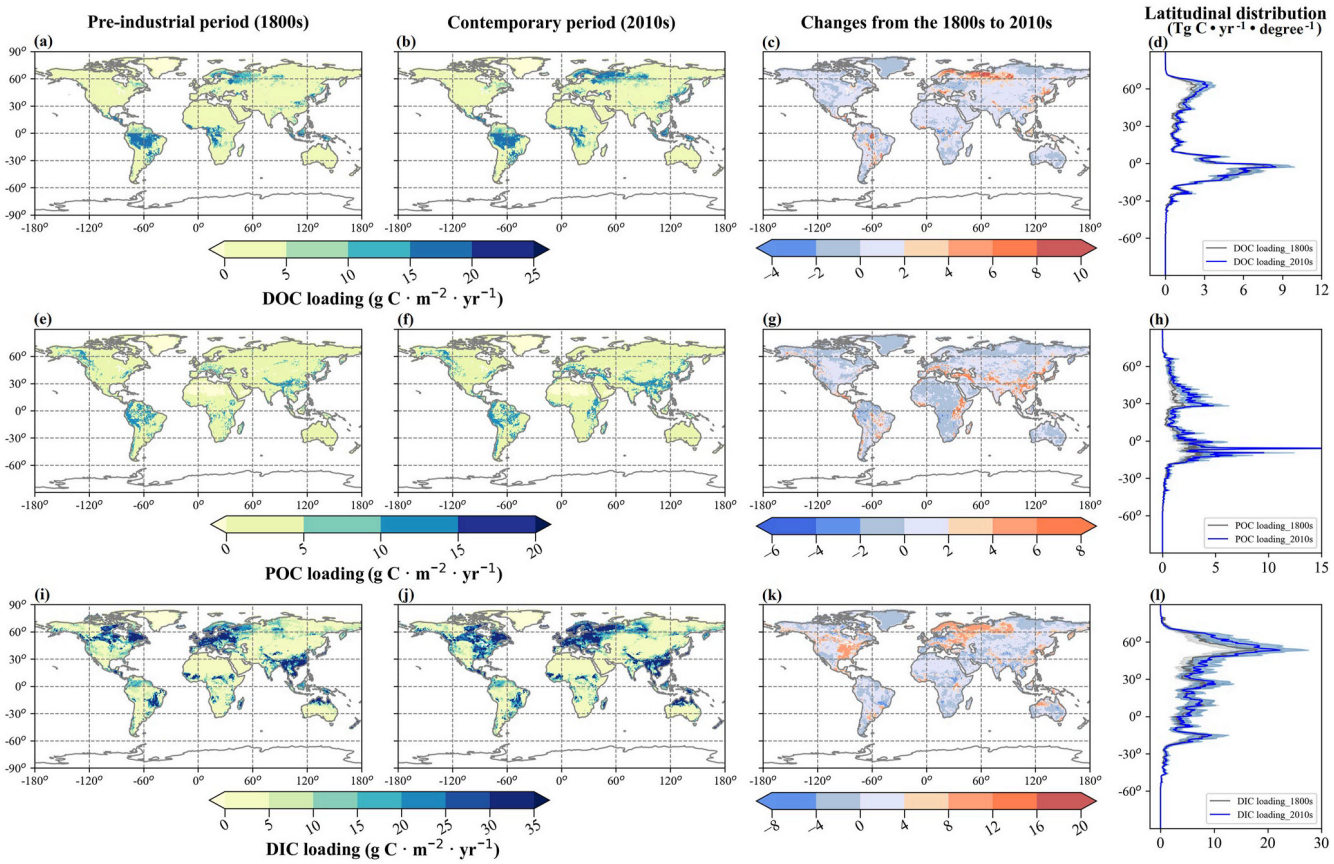

Figure 6. Spatial patterns of terrestrial dissolved organic carbon (top row), particulate organic carbon (middle row), and dissolved inorganic carbon (bottom row) loadings in the preindustrial period (1800s), and the contemporary period (2010s), and the change from the 1800s to the 2010s (third column). The fourth column shows the latitudinal averages of the loadings in the 1800s and 2010s (the shading area indicate uncertainty ranges with ±1 standard deviation).

5. Discussion

5.1. Comparison to Previous Studies

The C fluxes estimated by DLEM-TAC fall within the ranges given by previous studies, showing the consistency of this process-based model with other approaches, which are mostly data-driven (Table 2). DLEM-TAC DOC export (averaging 262 ± 33 Tg C yr^{-1} in the 2010s) is in good agreement with six previous studies, which ranged from 171 to 246 Tg C yr^{-1} (Table 2). The estimation of global DOC loading of about 280 Tg C yr^{-1} reported by Dai et al. (2012) and Nakhavali et al. (2020) is consistent with our estimate (averaging about 431 Tg C yr^{-1} in the 2010s) after the C loading from organic soil C is accounted for (around 170 Tg C yr^{-1}, as reported by Nakhavali et al. (2020)). The significant increasing trend of global DOC export from 1950 to 2019 simulated by DLEM-TAC is consistent with the finding of the Global NEWS model (Seitzinger et al., 2005) but contrasts with the report by M. Li et al. (2019), who claimed a decreasing trend in global DOC export. Nevertheless, DLEM-TAC simulations agree well with the results by M. Li et al. (2019) that DOC export showed a statistically significant increase in tropical regions (see also Lauerwald et al. (2020)). In contrast with the results by M. Li et al. (2019), DLEM-TAC estimated slight increases in arctic DOC export, which is supported by Bowring et al. (2020). A possible reason for such a difference is that the representations of impacts of freeze-thaw cycles are different, which would cause an increase in C loading in recent studies (Rawlins et al., 2021). To address this issue, more observations are needed to constrain the models. Similarly, DLEM-TAC POC export (154 ± 25 Tg C yr^{-1} in the 2010s) and DIC export (453 ± 94 Tg C yr^{-1} in the 2010s) are in line with the mean of previous studies (196 Tg C yr^{-1} for POC and 413 Tg C yr^{-1} for DIC) (Table 2). The significant increase in DIC export from 1960 to 2019 revealed by DLEM-TAC is supported by a previous data synthesis (M. Li et al., 2017). We should note that, our estimated burial C in rivers is slightly higher than that in lakes and reservoirs, due to the high deposition rate within river floodplains.

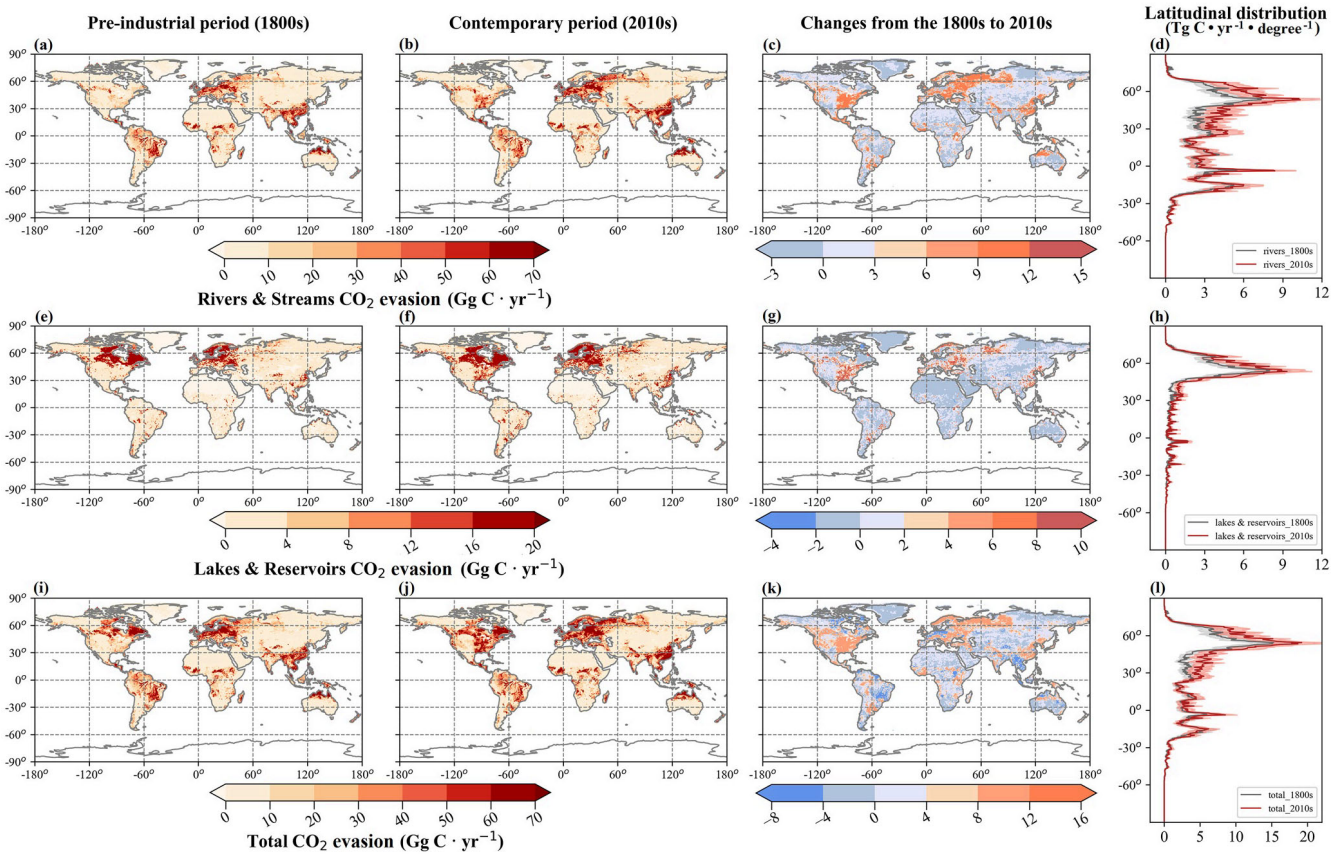

Figure 7. Spatial patterns and latitudinal distribution of riverine CO_2 (top), lacustrine CO_2 (middle), and all inland water CO_2 (bottom) evasion in the preindustrial period (1800s) and the contemporary period (2010s), and the change from the 1800s to the 2010s (third column). The fourth column shows the latitudinal averages of the loadings in the 1800s and 2010s (the shading area indicate uncertainty ranges with ±1 standard deviation).

Excluding PIC, the total C export estimated by DLEM-TAC (869 ± 151 Tg C yr^{-1} in the 2010s) is close to that estimated by Bauer et al. (2013) (Table 2). However, DLEM-TAC estimation of total C export is still larger than the one given by Resplandy et al. (2018) because their estimate only accounts for part of the river C export that is outgassed back to the ocean, which does not include the buried fraction (Table 2). The difference may be due to the C loss in estuaries (burial and outgassing), which occurs between the river outlet and the adjacent coastal ocean. Although the total terrestrial C loading given by DLEM-TAC (2281 ± 640 Tg C yr^{-1} in the 2010s) is much larger than the estimation provided by Cole et al. (2007) and is lower than those by Battin et al. (2023), several studies (Battin et al., 2009; Regnier et al., 2013) support our estimation (Table 2). The performances of the different methods in the estimation of riverine C exports and loadings need to be further evaluated in the future.

Our estimation of riverine CO_2 evasion was in the range of previous studies (Table 3). The riverine CO_2 evasion estimated by DLEM-TAC was around twice as much as the estimate by Cole et al. (2007) (Table 3), probably because their study ignored evasion from small rivers, which are now considered to be an important CO_2 source (M. Li et al., 2021). Our riverine CO_2 evasion is much lower than that given by Raymond et al. (2013) and S. Liu et al. (2022), with the estimated inland water CO_2 emission reached 2.5 Pg C yr^{-1}. Based on their calculation, the global land C loading can be larger than 3.4 Pg C yr^{-1} (inland water CO_2 emission plus global riverine export), which is 110% of the estimated C sink by the global terrestrial ecosystem (3.1 Pg C yr^{-1}) (Friedlingstein et al., 2022). However, the average fraction of leaching/net ecosystem exchange is about 20% for most of the observation sites in European sites (Kindler et al., 2011), which implies a potentially significant overestimation of inland water CO_2 emissions in the previous studies. The magnitude of lacustrine CO_2 evasion estimated by DLEM-TAC was higher than that of Cole et al. (2007), but lower than that of Raymond et al. (2013). The differences mainly arise from the tropical zone, since most of the observations were collected in the temperate and boreal regions. Hastie et al. (2018) reported a total CO_2 evasion of 272 Tg C yr^{-1} from lakes at high latitudes,

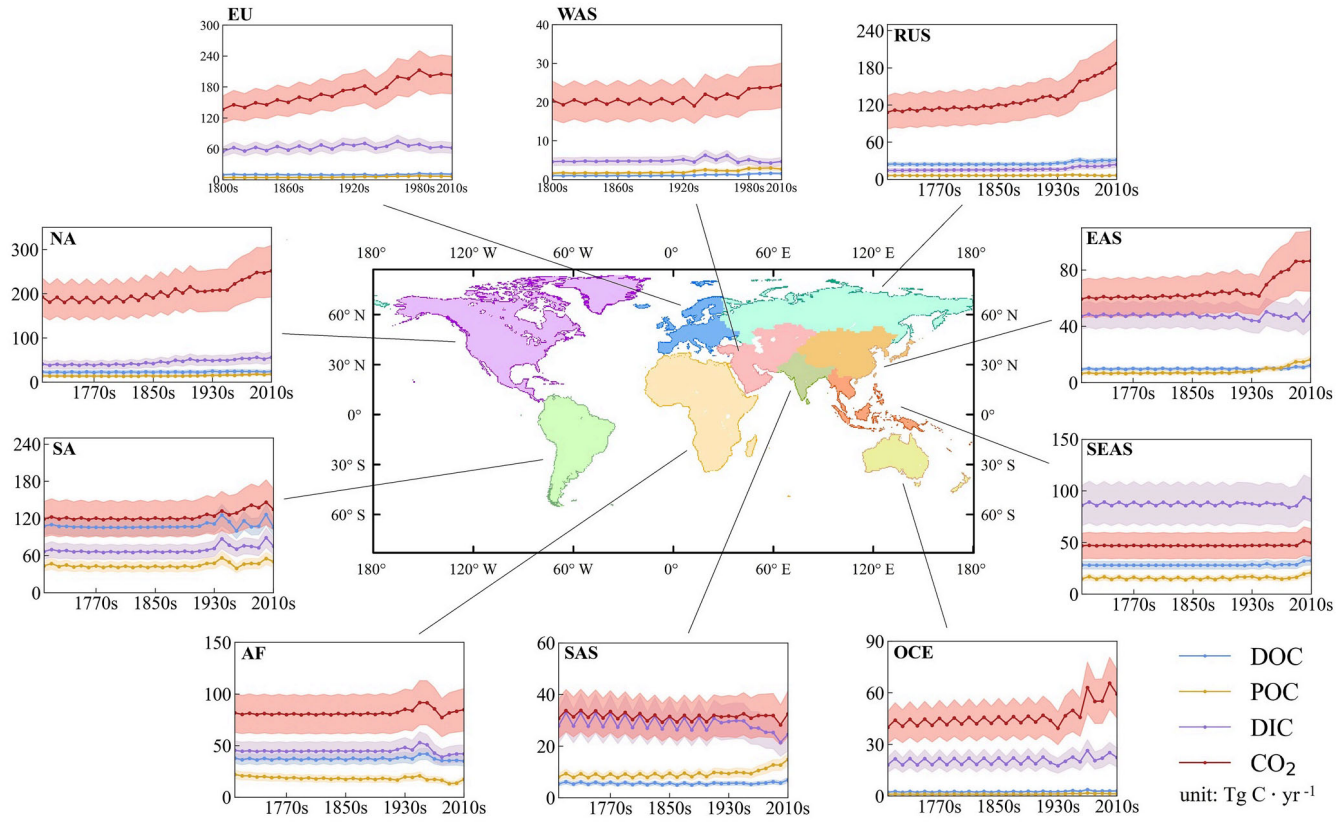

Figure 8. The temporal patterns of riverine carbon (dissolved organic carbon, particulate organic carbon, and dissolved inorganic carbon) exports and CO_2 evasion from inland water systems in 10 regions (NA: North America; EU: Europe; WAS: West Asia; RUS: Russia; EAS: East Asia; SEAS: Southeast Asia; OCE: Oceania; SAS: East Asia; AF: Africa; and SA: South America.). Note that the shading areas represent decadal variations with ±1 standard deviation.

which is almost equal to our estimate for the CO_2 evasion from global lakes. A reason for such a difference is that the lake area they used was much larger than that used in our study (Messager et al., 2016). The CO_2 evasion from reservoirs presented here is similar to the data synthesis estimate from Deemer et al. (2016), but far lower than that of St. Louis et al. (2000) because of their overestimation of global reservoir surface area (Johnson et al., 2021).

The global CO_2 evasion from inland waters in this study is close to the empirical estimations (Deng et al., 2022). Our simulated CO_2 evasion in the 2010s for most 106 river basins is comparable to their empirical estimates. Nevertheless, our estimates of CO_2 evasion from the Amazon and Congo Basins are lower than those of Deng et al. (2022) and Byrne et al. (2023) (Figure S5 in Supporting Information S1). This is because we do not consider the CO_2 evasion from wetlands and floodplains in our estimation, which are considered as the dominant source of CO_2 evasion from surface water in these two basins (Borges et al., 2015; Richey et al., 2002). Furthermore, inland water CO_2 evasions as well as the riverine C exports from Europe we estimated are much higher than those presented by H. Zhang et al. (2022). It is worth noting, however, that our estimations regarding European riverine C exports aligned closely with the magnitude documented in another global study (M. Li et al., 2017). We showed much lower CO_2 evasions in comparison to those by S. Liu et al. (2022). Our study may underestimate CO_2 evasions from rivers in mountainous regions such as the Rocky Mountains, the Andes, and the Himalayas, considering the high gas transfer velocity documented in S. Liu et al. (2022)'s study. These differences also suggest critical needs to better understand processes controlling C dynamics along the land-aquatic interface as well as better represent these processes in our model. To enhance the credibility of projections concerning inland water C fluxes on a global scale, it is imperative that future projection endeavors to prioritize the harmonization of results obtained from both global and regional studies, particularly within targeted regions. From the pre-industrial period to the recent decade, our increased rates of terrestrial C loading (25%), riverine C export (14%), and CO_2 evasion (32%) are in good agreement with the results reported by Regnier et al. (2022) (26% for terrestrial C loading, 12% for riverine C export, and 28% for CO_2 evasion).

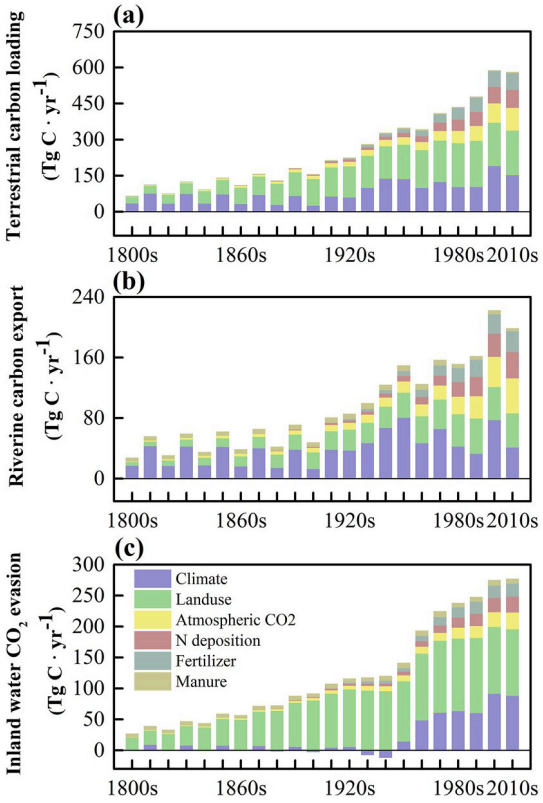

Figure 9. Decomposition of the factors influencing the long-term changes of (a) terrestrial carbon loading, (b) riverine carbon export, and (c) inland water CO_2 evasion from the 1800s to the 2010s.

5.2. Natural and Anthropogenic Drivers of the Changes in Inland Water Carbon Fluxes

The inter-decadal variations in model-simulated inland water C fluxes are mainly controlled by climate-related variability (Figure 9). Changes in precipitation and air temperature can directly affect ecosystem production and thus the C input to soil (Cleveland et al., 2011; Z. Zhang et al., 2016). Simultaneously, the shifts in precipitation patterns can largely alter runoff and further impact soil leaching and C transport in inland waters (Lal, 2005).

Climate variation together with elevated CO_2 significantly promoted vegetation growth and thus increased C loss from land to inland waters (P. Li et al., 2017). However, our modeling results showed that the contemporary DIC export is comparable to its pre-industrial level, which is supported by evidence derived from observations (Raymond & Hamilton, 2018). This is because stream water temperature is strongly correlated with air temperature (Mohseni et al., 1998, 1999), the increase in which would increase organic matter decomposition, accelerate gas exchange rates, and substantially increase CO_2 evasions in waters.

The estimated POC export increased substantially from 1900 to 2019, primarily due to land-use change. Most of the increase in POC export occurs in regions where a large area of cropland is converted from forest (Figures S1 and S8 in Supporting Information S1). This is because the erodibility of croplands is much higher than that of forests and grasslands (Williams & Berndt, 1977) leading to rapid loss of POC accumulated previously. The considerable increase in POC export in the arctic region can be mainly attributed to the high sensitivity of the ecosystems to climate change (Hilton et al., 2015) (Figure 9 and Figure S8 in Supporting Information S1).

Overall, nitrogen inputs including nitrogen deposition, nitrogen fertilizer and manure nitrogen applications are positively correlated with riverine C fluxes. We observed a notable increase in nitrogen effect on riverine C fluxes, specifically in recent years, in response to the consistent increasing rates of nitrogen deposition and nitrogen applications. In theory, the nitrogen inputs can alleviate the vegetation nitrogen limitation of global terrestrial ecosystems (Vitousek & Howarth, 1991), which contributes to the increased primary production, soil C pools and the associated C loadings from land to inland waters.

5.3. Significance of Inland Water Carbon Fluxes to the Global Carbon Budget

Increased evidence indicates that aquatic C fluxes need to be accounted for in revisions of the overall C balance of the terrestrial ecosystem (Cole et al., 2007; Friedlingstein et al., 2019). Constrained by fossil fuel emissions, atmospheric CO_2 growth rate, and C fluxes within fresh and salt water ecosystems, the global net CO_2 sink by terrestrial vegetation was estimated to be 2.2 Pg C yr^{-1} in the recent decade (Regnier et al., 2022). Our study indicated that inland water recycles and exports nearly half of the net land C sink into the atmosphere and ocean, highlighting the important role of inland waters in the global land C balance, an amount that should be taken into account in future C budgets. In addition, riverine C export is likely to provide substantial substrate to support microbial activity in the ocean and is an important term in the coastal C budget (Barrón & Duarte, 2015).

Based on our reconstruction of historical C fluxes between atmosphere, land, and water, lateral C fluxes in the pre-industrial period were found to be considerable. The anthropogenic activity has likely perturbed lateral C fluxes in the land-ocean aquatic continuum (LOAC), but this perturbation has been difficult to quantify (Regnier et al., 2022). Our work has quantified the long-term anthropogenic perturbation of lateral C fluxes and found a notable increase (25%) of C transfer from land to inland waters since the pre-industrial period, which intensified inland water CO_2 evasion, and to a lesser extent, export to the ocean. The global C budget of the Global Carbon Project assumed that the C fluxes in the LOAC have not changed since pre-industrial time (Friedlingstein et al., 2021). In contrast, we have highlighted the influence of multiple anthropogenic perturbations on lateral C

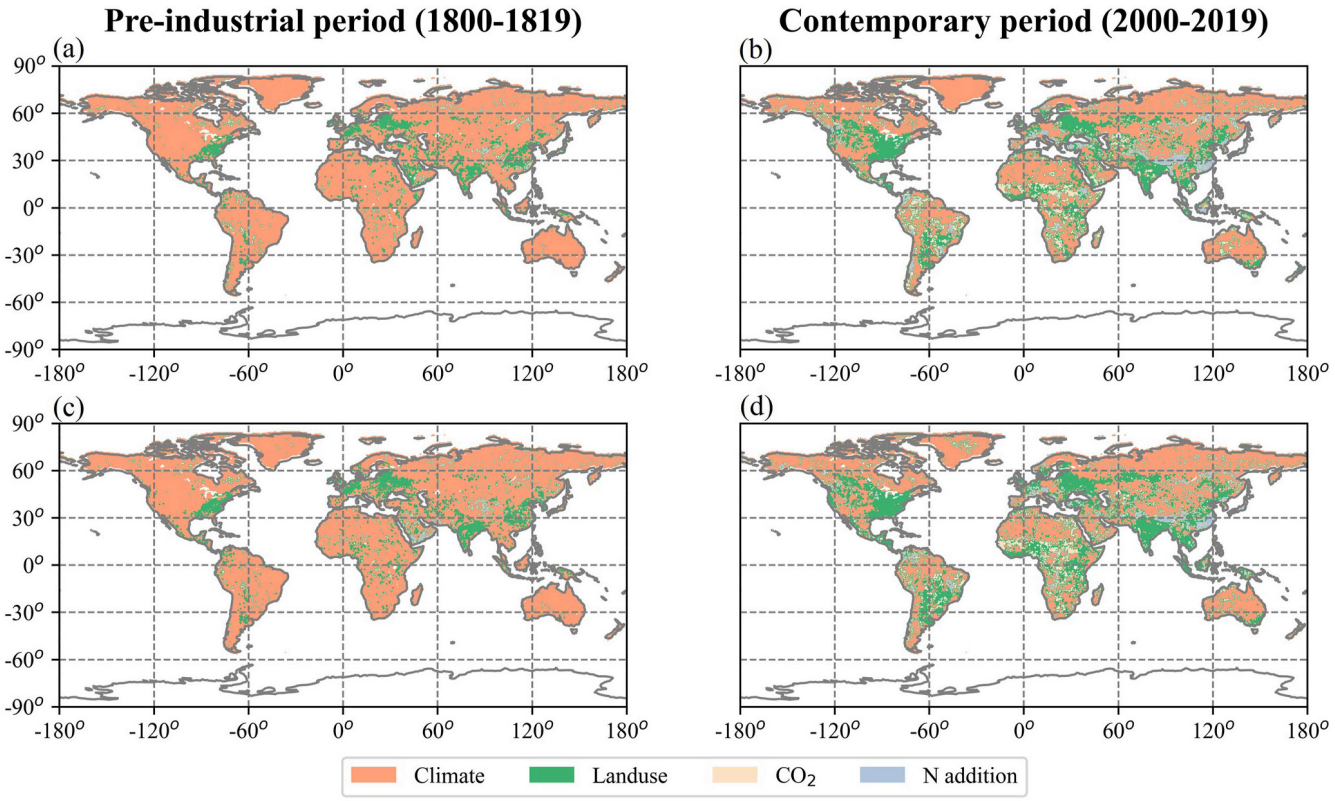

Figure 10. The dominant impact factors on terrestrial carbon loading (a, b) and inland water CO_2 evasion (c, d) in the early 19th century (1800–1819) and the early 21st century (2000–2019). The factor that caused the maximum changes is shown in each grid. Nitrogen addition includes nitrogen deposition and the application of nitrogen fertilizer and manure nitrogen.

fluxes, which should be considered for a robust quantification of the modern global C cycle and climate change mitigation (Regnier et al., 2013; Yvon-Durocher et al., 2012).

5.4. Uncertainty and Future Research

A major source of uncertainty in the estimation of inland water C fluxes is associated with the input data. For instance, the absence of seasonal variations in the spatial distribution of nitrogen inputs, including atmospheric nitrogen deposition, fertilizer and manure applications, may bias the estimation, as the timing of N inputs has substantial effects on land C and nitrogen cycles (Scharf et al., 2002). Similarly, the atmospheric CO_2 concentration is fixed throughout the year. In fact, atmospheric CO_2 is unevenly distributed across the globe and seasons (Keeling et al., 1989). In this study, we used a static global pH map for calculating CO_2 concentration in aquatic systems, which may introduce uncertainties by ignoring the temporal changes of pH level over time (Stets et al., 2014). In this study, we used five simulated river water surface areas as the uncertainty range, where values (0.73–0.81) close to those of Allen and Pavelsky (2018) can be considered the most robust one. However, the estimates of river water surface area still suffer great uncertainty due to the limit of spatial resolution of remote sensing products. The alteration of surface water area resulting from climate variability and extensive human activities holds considerable implications for inland water CO_2 evasions. For instance, our estimations reveal a contrasting trend in the upward trajectory of inland water CO_2 evasions in East Asia over recent decades compared to a previous study (Ran et al., 2021). This disparity can be attributed to the limitations of using static river data sets, needing to account for the declining riverine area in China during this period. Therefore, a global dynamic inland water network should be a critical task for future research. Additionally, other driving forces, including long-term climate variables and land-use change, are also limited by spatial resolution and data availability.

Uncertainties can also arise from model parameterization and the model structure. Compared to the major component of current Earth system models that can be used to simulate C flux in inland waters, DLEM-TAC is the most

Table 2
Comparison of Various Estimates on Global Carbon Exports From Rivers to Oceans

Carbon exports and references	Methods	Loadings	Exports
Dissolved organic carbon			
Cai (2011)	Data ensemble		246
Dai et al. (2012)	Meta-analysis	280	171
M. Li et al. (2017) and P. Li et al. (2017)	Empirical model		240
M. Li et al. (2019)	Processed-based		235
Mayorga et al. (2010)	Hybrid model[a]		187
Meybeck (1982)	Meta-analysis		216
Nakhavali et al. (2020)	Processed-based	280	
This study	Processed-based	428 ± 74	262 ± 33
Particulate organic carbon			
Beusen et al. (2005)	Empirical model		197
Cai (2011)	Data ensemble		216
M. Li et al. (2017) and P. Li et al. (2017)	Empirical model		240
Mayorga et al. (2010)	Hybrid model[a]		146
Meybeck (1982)	Data ensemble		180
Richey (2004)	Data ensemble	400 – 1400	
This study	Process-based	376 ± 114	154 ± 25
Dissolved inorganic carbon			
Cai (2011)	Data ensemble		407
Kempe (1979)	Data ensemble		454
M. Li et al. (2017) and P. Li et al. (2017)	Empirical model		410
Bauer et al. (2013)	Data ensemble		400
Meybeck (1982)	Data ensemble		396
Battin et al. (2023)	Meta-analysis	2440	
This study	Process-based	1477 ± 94	453 ± 94
Total			
Andersson et al. (2005)	Box model		950
Battin et al. (2009)	Data ensemble	1900	
Cole et al. (2007)	Meta-analysis	900	
M. Li et al. (2017) and P. Li et al. (2017)	Empirical model		1060[b]
Meybeck (1993)	Meta-analysis		960[b]
Regnier et al. (2013)	Data ensemble	2400	
Resplandy et al. (2018)	Top-down approach[c]		780
Bauer et al. (2013)	Data ensemble		850
Schlesinger and Melack (1981)	Data ensemble		400[d]
Regnier et al. (2022)	Data ensemble	2950 ± 550	950 ± 150
Battin et al. (2023)	Meta-analysis	720[e]	
Battin et al. (2023)	Meta-analysis	3,160	
This study	Process-based	2281 ± 640	869 ± 151

Note. The unit of the inland water carbon fluxes is Tg C $\cdot yr^{-1}$. DLEM-TAC estimates were averaged from 2010 to 2019.
[a]Global NEWS model is a hybrid of empirical, statistical, and mechanistic components. [b]Particulate inorganic carbon (168 Tg C $\cdot yr^{-1}$) was included in the estimates of total C exports. [c]Resplandy et al. (2018) used heat transport to constrain riverine carbon exports. [d]Total organic carbon only. [e]The value only encompasses the loading of DOC and POC.

Table 3
Comparison of Various Estimates of Global CO_2 Evasion From Inland Water Systems

Inland water CO_2 evasion and reference	Methods	Evasion
Rivers		
Aufdenkampe et al. (2011)	Data ensemble	560
Cole et al. (2007)	Meta-analysis	270[a]
Lauerwald et al. (2015)	Statistical model	650
Raymond et al. (2013)	Statistical model	1800
S. Liu et al. (2022)	Data ensemble	2000
Lauerwald et al. (2023b)	Data ensemble	1223
This study	Process-based	777 ± 179
Lakes		
Cole et al. (2007)	Meta-analysis	110
Raymond et al. (2013)	Statistical model	292
Lauerwald et al. (2023b)	Data ensemble	205[b]
This study	Process-based	304 ± 65
Reservoirs		
Deemer et al. (2016)	Data ensemble	37
St. Louis et al. (2000)	Data ensemble	1000
Lauerwald et al. (2023b)	Data ensemble	191
This study	Process-based	33 ± 8
Total		
Aufdenkampe et al. (2011)	Data ensemble	1200
Cole et al. (2007)	Meta-analysis	750[a]
Raymond et al. (2013)	Statistical model	2120
Regnier et al. (2022)	Data ensemble	1,850 ± 500
Lauerwald et al. (2023b)	Data ensemble	1,513
This study	Process-based	1,113 ± 251

Note. The unit of the inland water CO_2 evasion is Tg C $\cdot yr^{-1}$.
[a]This study only analyzed evasion from large rivers. [b]The value includes CO_2 evasion from natural lakes and the lakes with dams.

comprehensive model that fully couples aquatic and land processes by incorporating all the inland water types (river, lake and reservoir) with explicit representation of small stream and large rivers. DLEM-TAC has the ability in simulating three carbon species (DOC, DIC and POC) as well as inland water CO_2 evasion (Table S3 in Supporting Information S1). However, the parameters relevant to the aquatic biogeochemical reaction rates in inland waters, such as the organic matter decomposition rate, particle deposition rate, and CO_2 air-water exchange velocity, are largely fixed for all river systems in our simulation. Although our parameter values fall into the ranges of previous studies, the parameters likely vary across river systems. For instance, S. Liu et al. (2022) demonstrated the substantial seasonal variability of gas transfer velocity across different climate zones. Moreover, their study also highlighted the intricate and non-linear association between gas transfer velocity and basin conditions, such as terrain and gas exchange patterns. Employing a very coarse empirical model for the estimation of CO_2 gas transfer velocity may introduce significant errors, particularly in streams characterized by steep terrain. More monitoring sites located within headwater zones are needed to better constrain these parameters. In addition, the current model still lacks a full representation of hydrodynamics and C-associated biogeochemistry although much progress has been made. For instance, a better representation of carbon dynamics in hillslope and groundwater would significantly influence the ratio of inorganic carbon over organic carbon, especially in riparian and hyporheic zones, which need more observations to support the algorithm design and parametrization. Also, we do not consider the vertical stratification of lakes and reservoirs, and the associated carbon reaction and CH_4 flux, which requires systematic observations to quantify the carbon fluxes of multiple interfaces.

6. Conclusion

In this study, the DLEM-TAC model, which integrates both land and aquatic C processes, was applied to quantify the global inland water C budget from 1800 to 2019. Based on our DLEM-TAC estimates over recent decades, we estimate that around 2.3 Pg C yr^{-1} entered inland water ecosystems in the 2010s, and a major proportion of C loading was eventually emitted by inland waters to the atmosphere as CO_2 (1.1 Pg C yr^{-1}) and exported to the oceans by rivers (0.9 Pg C yr^{-1}). Under anthropogenic disturbances, a large increase in terrestrial C loading produced a corresponding increase in CO_2 evasion from inland waters from the 1800s to 2010s. A sustained increase in the exports of DIC, DOC, and POC as well as CO_2 evasion can be attributed to climate change, land-use change, and N application. Although uncertainties exist, our results suggest that inland water C dynamics play a critical role in the global C budget. Our study indicated that inland water recycles and exports nearly half of the net land C sink into the atmosphere and oceans, highlighting the important role of inland waters in the global land C balance, an amount that should be taken into account in future C budget assessment. More observations in headwater zones, arctic regions, and improved process-based modeling tools are needed to better constrain the estimates of inland water C fluxes.

Data Availability Statement

The CRU-NCEP data are freely available at https://vesg.ipsl.upmc.fr. NOAA GLOBALVIEW-CO2 data are available at https://www.esrl.noaa.gov. The required hydrological data are available at http://files.ntsg.umt.edu/data/DRT/upscaled_global_hydrography/ (Dominant River Tracing data set), http://www.horizon-systems.com/NHDPlus/index.php (National Hydrography data set plus v2 data), https://www.hydrosheds.org/products/hydrolakes (HydroLAKES data set), and https://sedac.ciesin.columbia.edu/data/collection/grand-v1 (GRanD v1.01 database), respectively.

Acknowledgments
This study has been supported by the NASA (Grant NNX12AP84G, NNX14AO73G, NNX10AU06G, NNX11AD47G, and NNX14AF93G), National Science Foundation (Grant 1210360 and 1243232), NOAA (Grant NA16NOS4780207 and NA16NOS4780204), and U.S. Department of Treasury (DISL-MESC-AL-COE-06). The data sets relevant to this study are archived in the International Center for Climate and Global Change Research at Auburn University (https://auburn.box.com/v/GLinlandwatercarbon). LRL and HYL were supported by the E3SM project funded by the Office of Science, U.S. Department of Energy Biological and Environmental Research as part of the Earth System Model Development (ESMD) program area. Pacific Northwest National Laboratory is operated for U.S. Department of Energy by Battelle Memorial Institute under Contract DE-AC05-76RL01830.

References

Allen, G. H., & Pavelsky, T. M. (2018). Global extent of rivers and streams. *Science*, *361*(6402), 585–588. https://doi.org/10.1126/science.aat0636

Andersson, A. J., Mackenzie, F. T., & Lerman, A. (2005). Coastal ocean and carbonate systems in the high CO_2 world of the Anthropocene. *American Journal of Science*, *305*(9), 875–918. https://doi.org/10.2475/ajs.305.9.875

Aufdenkampe, A. K., Mayorga, E., Raymond, P. A., Melack, J. M., Doney, S. C., Alin, S. R., et al. (2011). Riverine coupling of biogeochemical cycles between land, oceans, and atmosphere. *Frontiers in Ecology and the Environment*, *9*(1), 53–60. https://doi.org/10.1890/100014

Barrón, C., & Duarte, C. M. (2015). Dissolved organic carbon pools and export from the coastal ocean. *Global Biogeochemical Cycles*, *29*(10), 1725–1738. https://doi.org/10.1002/2014GB005056

Bastviken, D., Tranvik, L. J., Downing, J. A., Crill, P. M., & Enrich-Prast, A. (2011). Freshwater methane emissions offset the continental carbon sink. *Science*, *331*(6013), 50. https://doi.org/10.1126/science.1196808

Battin, T. J., Kaplan, L. A., Findlay, S., Hopkinson, C. S., Marti, E., Packman, A. I., et al. (2008). Biophysical controls on organic carbon fluxes in fluvial networks. *Nature Geoscience*, *1*(2), 95–100. https://doi.org/10.1038/ngeo101

Battin, T. J., Lauerwald, R., Bernhardt, E. S., Bertuzzo, E., Gener, L. G., Hall, R. O., Jr., et al. (2023). River ecosystem metabolism and carbon biogeochemistry in a changing world. *Nature*, *613*(7944), 449–459. https://doi.org/10.1038/s41586-022-05500-8

Battin, T. J., Luyssaert, S., Kaplan, L. A., Aufdenkampe, A. K., Richter, A., & Tranvik, L. J. (2009). The boundless carbon cycle. *Nature Geoscience*, *2*(9), 598–600. https://doi.org/10.1038/ngeo618

Bauer, J. E., Cai, W.-J., Raymond, P. A., Bianchi, T. S., Hopkinson, C. S., & Regnier, P. A. (2013). The changing carbon cycle of the coastal ocean. *Nature*, *504*(7478), 61–70. https://doi.org/10.1038/nature12857

Beusen, A. H. W., Dekkers, A. L. M., Bouwman, A. F., Ludwig, W., & Harrison, J. (2005). Estimation of global river transport of sediments and associated particulate C, N, and P. *Global Biogeochemical Cycles*, *19*(4), GB4S05. https://doi.org/10.1029/2005gb002453

Biemans, H., Haddeland, I., Kabat, P., Ludwig, F., Hutjes, R., Heinke, J., et al. (2011). Impact of reservoirs on river discharge and irrigation water supply during the 20th century. *Water Resources Research*, *47*(3), W03509. https://doi.org/10.1029/2009WR008929

Borges, A. V., Darchambeau, F., Teodoru, C. R., Marwick, T. R., Tamooh, F., Geeraert, N., et al. (2015). Globally significant greenhouse-gas emissions from African inland waters. *Nature Geoscience*, *8*(8), 637–642. https://doi.org/10.1038/ngeo2486

Bowring, S. P., Lauerwald, R., Guenet, B., Zhu, D., Guimberteau, M., Regnier, P., et al. (2020). ORCHIDEE MICT-LEAK (r5459), a global model for the production, transport, and transformation of dissolved organic carbon from Arctic permafrost regions–Part 2: Model evaluation over the Lena River basin. *Geoscientific Model Development*, *13*(2), 507–520. https://doi.org/10.5194/gmd-13-507-2020

Butman, D., & Raymond, P. A. (2011). Significant efflux of carbon dioxide from streams and rivers in the United States. *Nature Geoscience*, *4*(12), 839–842. https://doi.org/10.1038/ngeo1294

Butman, D., Stackpoole, S., Stets, E., McDonald, C. P., Clow, D. W., & Striegl, R. G. (2016). Aquatic carbon cycling in the conterminous United States and implications for terrestrial carbon accounting. *Proceedings of the National Academy of Sciences of the United States of America*, *113*(1), 58–63. https://doi.org/10.1073/pnas.1512651112

Byrne, B., Baker, D. F., Basu, S., Bertolacci, M., Bowman, K. W., Carroll, D., et al. (2023). National CO_2 budgets (2015–2020) inferred from atmospheric CO_2 observations in support of the Global Stocktake. *Earth System Science Data*, *15*(2), 1–59. https://doi.org/10.5194/essd-15-963-2023

Cai, W. J. (2011). Estuarine and coastal ocean carbon paradox: CO_2 sinks or sites of terrestrial carbon incineration? *Annual Review of Marine Science*, *3*(1), 123–145. https://doi.org/10.1146/annurev-marine-120709-142723

Chow, V. T. (1964). A compendium of water-resources technology, Ven Te Chow. In *Handbook of applied hydrology* (pp. 8–61).

Ciais, P., Bastos, A., Chevallier, F., Lauerwald, R., Poulter, B., Canadell, J. G., et al. (2022). Definitions and methods to estimate regional land carbon fluxes for the second phase of the REgional Carbon Cycle Assessment and Processes Project (RECCAP-2). *Geoscientific Model Development*, *15*(3), 1289–1316. https://doi.org/10.5194/gmd-15-1289-2022

Cleveland, C. C., Townsend, A. R., Taylor, P., Alvarez-Clare, S., Bustamante, M. M., Chuyong, G., et al. (2011). Relationships among net primary productivity, nutrients and climate in tropical rain forest: A pan-tropical analysis. *Ecology Letters*, *14*(9), 939–947. https://doi.org/10.1111/j.1461-0248.2011.01658.x

Cole, J. J., Prairie, Y. T., Caraco, N. F., McDowell, W. H., Tranvik, L. J., Striegl, R. G., et al. (2007). Plumbing the global carbon cycle: Integrating inland waters into the terrestrial carbon budget. *Ecosystems*, *10*(1), 172–185. https://doi.org/10.1007/s10021-006-9013-8

Dai, M., Yin, Z., Meng, F., Liu, Q., & Cai, W.-J. (2012). Spatial distribution of riverine DOC inputs to the ocean: An updated global synthesis. *Current Opinion in Environmental Sustainability*, *4*(2), 170–178. https://doi.org/10.1016/j.cosust.2012.03.003

Deemer, B. R., Harrison, J. A., Li, S., Beaulieu, J. J., DelSontro, T., Barros, N., et al. (2016). Greenhouse gas emissions from reservoir water surfaces: A new global synthesis. *BioScience*, *66*(11), 949–964. https://doi.org/10.1093/biosci/biw117

Deng, Z., Ciais, P., Tzompa-Sosa, Z. A., Saunois, M., Qiu, C., Tan, C., et al. (2022). Comparing national greenhouse gas budgets reported in UNFCCC inventories against atmospheric inversions. *Earth System Science Data*, *14*(4), 1639–1675. https://doi.org/10.5194/essd-14-1639-2022

Fekete, B. M., Vörösmarty, C. J., & Lammers, R. B. J. W. R. R. (2001). Scaling gridded river networks for macroscale hydrology: Development, analysis, and control of error. *Water Resources Research*, *37*(7), 1955–1967. https://doi.org/10.1029/2001wr900024

Findlay, S. E. (2005). Increased carbon transport in the Hudson river: Unexpected consequence of nitrogen deposition? *Frontiers in Ecology and the Environment*, *3*(3), 133–137. https://doi.org/10.1890/1540-9295(2005)003[0133:ICTITH]2.0.CO;2

Friedlingstein, P., Jones, M. W., O'Sullivan, M., Andrew, R. M., Bakker, D. C., Hauck, J., et al. (2021). Global carbon budget 2021. *Earth System Science Data*, *14*(4), 1917–2005. https://doi.org/10.5194/essd-14-1917-2022

Friedlingstein, P., Jones, M. W., O'sullivan, M., Andrew, R. M., Bakker, D. C., Hauck, J., et al. (2022). Global carbon budget 2021. *Earth System Science Data*, *14*(4), 1917–2005. https://doi.org/10.5194/essd-14-1917-2022

Friedlingstein, P., Jones, M. W., O'sullivan, M., Andrew, R. M., Hauck, J., Peters, G. P., et al. (2019). Global carbon budget 2019. *Earth System Science Data*, *11*(4), 1783–1838. https://doi.org/10.5194/essd-11-1783-2019

Galy, V., Peucker-Ehrenbrink, B., & Eglinton, T. (2015). Global carbon export from the terrestrial biosphere controlled by erosion. *Nature*, *521*(7551), 204–207. https://doi.org/10.1038/nature14400

Getirana, A. C., Boone, A., Yamazaki, D., Decharme, B., Papa, F., & Mognard, N. (2012). The hydrological modeling and analysis platform (HyMAP): Evaluation in the Amazon basin. *Journal of Hydrometeorology*, *13*(6), 1641–1665. https://doi.org/10.1175/JHM-D-12-021.1

Girardin, M. P., Raulier, F., Bernier, P. Y., & Tardif, J. C. (2008). Response of tree growth to a changing climate in boreal central Canada: A comparison of empirical, process-based, and hybrid modelling approaches. *Ecological Modelling*, *213*(2), 209–228. https://doi.org/10.1016/j.ecolmodel.2007.12.010

Haddeland, I., Skaugen, T., & Lettenmaier, D. P. (2006). Anthropogenic impacts on continental surface water fluxes. *Geophysical Research Letters*, *33*(8), L08406. https://doi.org/10.1029/2006GL026047

Hanasaki, N., Kanae, S., & Oki, T. (2006). A reservoir operation scheme for global river routing models. *Journal of Hydrology*, *327*(1–2), 22–41. https://doi.org/10.1016/j.jhydrol.2005.11.011

Hartmann, J., Lauerwald, R., & Moosdorf, N. (2019). GLORICH—Global river chemistry database, supplement to: Hartmann, J et al. (2014): A brief overview of the global river chemistry database, GLORICH. *Procedia Earth and Planetary Science*, *10*, 23–27. https://doi.org/10.1016/j.proeps.2014.08.005

Hastie, A., Lauerwald, R., Ciais, P., & Regnier, P. (2019). Aquatic carbon fluxes dampen the overall variation of net ecosystem productivity in the Amazon basin: An analysis of the interannual variability in the boundless carbon cycle. *Global Change Biology*, *25*(6), 2094–2111. https://doi.org/10.1111/gcb.14620

Hastie, A., Lauerwald, R., Weyhenmeyer, G., Sobek, S., Verpoorter, C., & Regnier, P. (2018). CO_2 evasion from boreal lakes: Revised estimate, drivers of spatial variability, and future projections. *Global Change Biology*, *24*(2), 711–728. https://doi.org/10.1111/gcb.13902

Hilton, R. G., Galy, V., Gaillardet, J., Dellinger, M., Bryant, C., O'Regan, M., et al. (2015). Erosion of organic carbon in the Arctic as a geological carbon dioxide sink. *Nature*, *524*(7563), 84–87. https://doi.org/10.1038/nature14653

Houghton, R. A. (2010). How well do we know the flux of CO_2 from land-use change? *Tellus B: Chemical and Physical Meteorology*, *62*(5), 337–351. https://doi.org/10.1111/j.1600-0889.2010.00473.x

Hu, M., Chen, D., & Dahlgren, R. A. (2016). Modeling nitrous oxide emission from rivers: A global assessment. *Global Change Biology*, *22*(11), 3566–3582. https://doi.org/10.1111/gcb.13351

Johnson, M. S., Matthews, E., Bastviken, D., Deemer, B., Du, J., & Genovese, V. (2021). Spatiotemporal methane emission from global reservoirs. *Journal of Geophysical Research: Biogeosciences*, *126*(8), e2021JG006305. https://doi.org/10.1029/2021JG006305

Keeling, C. D., Bacastow, R. B., Carter, A., Piper, S. C., Whorf, T. P., Heimann, M., et al. (1989). A three-dimensional model of atmospheric CO_2 transport based on observed winds: 1. Analysis of observational data. *Aspects of climate variability in the Pacific and the Western Americas*, *55*, 165–236. https://doi.org/10.1029/GM055p0165

Kempe, S. (1979). Carbon in the freshwater cycle. *The Global Carbon Cycle*, *13*, 317–342.

Kindler, R., Siemens, J., Kaiser, K., Walmsley, D. C., Bernhofer, C., Buchmann, N., et al. (2011). Dissolved carbon leaching from soil is a crucial component of the net ecosystem carbon balance. *Global Change Biology*, *17*(2), 1167–1185. https://doi.org/10.1111/j.1365-2486.2010.02282.x

Klein Goldewijk, K., Beusen, A., Doelman, J., & Stehfest, E. (2017). Anthropogenic land use estimates for the Holocene–HYDE 3.2. *Earth System Science Data*, *9*(2), 927–953. https://doi.org/10.5194/essd-9-927-2017

Kroeze, C., Dumont, E., & Seitzinger, S. P. (2005). New estimates of global emissions of N2O from rivers and estuaries. *Environmental Sciences*, *2*(2–3), 159–165. https://doi.org/10.1080/15693430500384671

Lal, R. (2005). Influence of soil erosion on carbon dynamics in the world. In *Soil erosion and carbon dynamics* (pp. 23–35). CRC Press.

Laudon, H., Buttle, J., Carey, S. K., McDonnell, J., McGuire, K., Seibert, J., et al. (2012). Cross-regional prediction of long-term trajectory of stream water DOC response to climate change. *Geophysical Research Letters*, *39*(18), L18404. https://doi.org/10.1029/2012GL053033

Lauerwald, R., Allen, G. H., Deemer, B. R., Liu, S., Maavara, T., Raymond, P., et al. (2023a). Inland water greenhouse gas budgets for RECCAP2: 1. State-of-the-art of global scale assessments. *Global Biogeochemical Cycles*, *37*(5), e2022GB007657. https://doi.org/10.1029/2022gb007657

Lauerwald, R., Allen, G. H., Deemer, B. R., Liu, S., Maavara, T., Raymond, P., et al. (2023b). Inland water greenhouse gas budgets for RECCAP2: 2. Regionalization and homogenization of estimates. *Global Biogeochemical Cycles*, *37*(5), e2022GB007658. https://doi.org/10.1029/2022gb007658

Lauerwald, R., Laruelle, G. G., Hartmann, J., Ciais, P., & Regnier, P. A. (2015). Spatial patterns in CO_2 evasion from the global river network. *Global Biogeochemical Cycles*, *29*(5), 534–554. https://doi.org/10.1002/2014GB004941

Lauerwald, R., Regnier, P., Guenet, B., Friedlingstein, P., & Ciais, P. (2020). How simulations of the land carbon sink are biased by ignoring fluvial carbon transfers: A case study for the Amazon basin. *One Earth*, *3*(2), 226–236. https://doi.org/10.1016/j.oneear.2020.07.009

Leach, J. A., & Moore, R. D. (2019). Empirical stream thermal sensitivities may underestimate stream temperature response to climate warming. *Water Resources Research*, *55*(7), 5453–5467. https://doi.org/10.1029/2018WR024236

Lehner, B., Liermann, C. R., Revenga, C., Vörösmarty, C., Fekete, B., Crouzet, P., et al. (2011). High-resolution mapping of the world's reservoirs and dams for sustainable river-flow management. *Frontiers in Ecology and the Environment*, *9*(9), 494–502. https://doi.org/10.1890/100125

Le Quéré, C., Andrew, R. M., Friedlingstein, P., Sitch, S., Hauck, J., Pongratz, J., et al. (2018). Global carbon budget 2018. *Earth System Science Data*, *10*(4), 2141–2194. https://doi.org/10.5194/essd-10-2141-2018

Li, H., Wigmosta, M. S., Wu, H., Huang, M., Ke, Y., Coleman, A. M., & Leung, L. R. (2013). A physically based runoff routing model for land surface and earth system models. *Journal of Hydrometeorology*, *14*(3), 808–828. https://doi.org/10.1175/JHM-D-12-015.1

Li, H.-Y., Leung, L. R., Getirana, A., Huang, M., Wu, H., Xu, Y., et al. (2015). Evaluating global streamflow simulations by a physically based routing model coupled with the community land model. *Journal of Hydrometeorology*, *16*(2), 948–971. https://doi.org/10.1175/jhm-d-14-0079.1

Li, M., Peng, C., Wang, M., Xue, W., Zhang, K., Wang, K., et al. (2017). The carbon flux of global rivers: A re-evaluation of amount and spatial patterns. *Ecological Indicators*, *80*, 40–51. https://doi.org/10.1016/j.ecolind.2017.04.049

Li, M., Peng, C., Zhang, K., Xu, L., Wang, J., Yang, Y., et al. (2021). Headwater stream ecosystem: An important source of greenhouse gases to the atmosphere. *Water Research*, *190*, 116738. https://doi.org/10.1016/j.watres.2020.116738

Li, M., Peng, C., Zhou, X., Yang, Y., Guo, Y., Shi, G., & Zhu, Q. (2019). Modeling global riverine DOC flux dynamics from 1951 to 2015. *Journal of Advances in Modeling Earth Systems*, *11*(2), 514–530. https://doi.org/10.1029/2018MS001363

Li, P., Peng, C., Wang, M., Li, W., Zhao, P., Wang, K., et al. (2017). Quantification of the response of global terrestrial net primary production to multifactor global change. *Ecological Indicators*, *76*, 245–255. https://doi.org/10.1016/j.ecolind.2017.01.021

Liu, M., & Tian, H. (2010). China's land cover and land use change from 1700 to 2005: Estimations from high-resolution satellite data and historical archives. *Global Biogeochemical Cycles*, *24*(3), GB3003. https://doi.org/10.1029/2009GB003687

Liu, S., Kuhn, C., Amatulli, G., Aho, K., Butman, D. E., Allen, G. H., et al. (2022). The importance of hydrology in routing terrestrial carbon to the atmosphere via global streams and rivers. *Proceedings of the National Academy of Sciences of the United States of America*, *119*(11), e2106322119. https://doi.org/10.1073/pnas.2106322119

Lu, C., & Tian, H. (2017). Global nitrogen and phosphorus fertilizer use for agriculture production in the past half century: Shifted hot spots and nutrient imbalance. *Earth System Science Data*, *9*(1), 181–192. https://doi.org/10.5194/essd-9-181-2017

Ludwig, W., Amiotte Suchet, P., & Probst, J.-L. (1996). River discharges of carbon to the world's oceans: Determining local inputs of alkalinity and of dissolved and particulate organic carbon. *Sciences de la terre et des planètes*, *323*, 1007–1014.

Marescaux, A., Thieu, V., Gypens, N., Silvestre, M., & Garnier, J. (2020). Modeling inorganic carbon dynamics in the Seine River continuum in France. *Hydrology and Earth System Sciences*, *24*(5), 2379–2398. https://doi.org/10.5194/hess-24-2379-2020

Mayorga, E., Seitzinger, S. P., Harrison, J. A., Dumont, E., Beusen, A. H., Bouwman, A., et al. (2010). Global nutrient export from WaterSheds 2 (NEWS 2): Model development and implementation. *Environmental Modelling & Software*, *25*(7), 837–853. https://doi.org/10.1016/j.envsoft.2010.01.007

McClain, M. E., Boyer, E. W., Dent, C. L., Gergel, S. E., Grimm, N. B., Groffman, P. M., et al. (2003). Biogeochemical hot spots and hot moments at the interface of terrestrial and aquatic ecosystems. *Ecosystems*, *6*(4), 301–312. https://doi.org/10.1007/s10021-003-0161-9

Messager, M. L., Lehner, B., Grill, G., Nedeva, I., & Schmitt, O. (2016). Estimating the volume and age of water stored in global lakes using a geo-statistical approach. *Nature Communications*, *7*(1), 1–11. https://doi.org/10.1038/ncomms13603

Meybeck, M. (1982). Carbon, nitrogen, and phosphorus transport by world rivers. *American Journal of Science*, *282*(4), 401–450. https://doi.org/10.2475/ajs.282.4.401

Meybeck, M. (1993). C, N, P and S in rivers: From sources to global inputs. In *Interactions of C, N, P and S biogeochemical cycles and global change* (pp. 163–193). Springer Berlin Heidelberg.

Meybeck, M., & Ragu, A. (2012). *GEMS-GLORI world river discharge database* (Vol. 10). Laboratoire de Géologie Appliquée, Université Pierre et Marie Curie.

Mohseni, O., Erickson, T. R., & Stefan, H. G. (1999). Sensitivity of stream temperatures in the United States to air temperatures projected under a global warming scenario. *Water Resources Research*, *35*(12), 3723–3733. https://doi.org/10.1029/1999wr900193

Mohseni, O., Stefan, H. G., & Erickson, T. R. (1998). A nonlinear regression model for weekly stream temperatures. *Water Resources Research*, *34*(10), 2685–2692. https://doi.org/10.1029/98wr01877

Moriasi, D. N., Gitau, M. W., Pai, N., & Daggupati, P. (2015). Hydrologic and water quality models: Performance measures and evaluation criteria. *Transactions of the ASABE*, *58*(6), 1763–1785.

Najjar, R. G., Herrmann, M., Alexander, R., Boyer, E. W., Burdige, D., Butman, D., et al. (2018). Carbon budget of tidal wetlands, estuaries, and shelf waters of Eastern North America. *Global Biogeochemical Cycles*, *32*(3), 389–416. https://doi.org/10.1002/2017gb005790

Nakayama, T. (2022). Impact of anthropogenic disturbances on carbon cycle changes in terrestrial-aquatic-estuarine continuum by using an advanced process-based model. *Hydrological Processes*, *36*(2), e14471. https://doi.org/10.1002/hyp.14471

Nakhavali, M., Lauerwald, R., Regnier, P., Guenet, B., Chadburn, S., & Friedlingstein, P. (2020). Leaching of dissolved organic carbon from mineral soils plays a significant role in the terrestrial carbon balance. *Global Change Biology*, *27*(5), 1083–1096. https://doi.org/10.1111/gcb.15460

Nash, J. E., & Sutcliffe, J. V. (1970). River flow forecasting through conceptual models part I—A discussion of principles. *Journal of Hydrology*, *10*(3), 282–290. https://doi.org/10.1016/0022-1694(70)90255-6

Pan, S., Bian, Z., Tian, H., Yao, Y., Najjar, R. G., Friedrichs, M. A. M., et al. (2021). Impacts of multiple environmental changes on long-term nitrogen loading from the Chesapeake Bay watershed. *Journal of Geophysical Research: Biogeosciences*, *126*(5), e2020JG005826. https://doi.org/10.1029/2020jg005826

Pastor, J., Solin, J., Bridgham, S. D., Updegraff, K., Harth, C., Weishampel, P., & Dewey, B. (2003). Global warming and the export of dissolved organic carbon from boreal peatlands. *Oikos*, *100*(2), 380–386. https://doi.org/10.1034/j.1600-0706.2003.11774.x

Ran, L., Butman, D. E., Battin, T. J., Yang, X., Tian, M., Duvert, C., et al. (2021). Substantial decrease in CO_2 emissions from Chinese inland waters due to global change. *Nature Communications*, *12*(1), 1730. https://doi.org/10.1038/s41467-021-21926-6

Rawlins, M. A., Connolly, C. T., & McClelland, J. W. (2021). Modeling terrestrial dissolved organic carbon loading to western Arctic rivers. *Journal of Geophysical Research: Biogeosciences*, *126*(10), e2021JG006420. https://doi.org/10.1029/2021jg006420

Raymond, P. A., & Hamilton, S. K. (2018). Anthropogenic influences on riverine fluxes of dissolved inorganic carbon to the oceans. *Limnology Oceanography Letters*, *3*(3), 143–155. https://doi.org/10.1002/lol2.10069

Raymond, P. A., Hartmann, J., Lauerwald, R., Sobek, S., McDonald, C., Hoover, M., et al. (2013). Global carbon dioxide emissions from inland waters. *Nature*, *503*(7476), 355–359. https://doi.org/10.1038/nature12760

Raymond, P. A., & Oh, N. H. (2007). An empirical study of climatic controls on riverine C export from three major US watersheds. *Global Biogeochemical Cycles*, *21*(2), GB2022. https://doi.org/10.1029/2006gb002783

Raymond, P. A., Zappa, C. J., Butman, D., Bott, T. L., Potter, J., Mulholland, P., et al. (2012). Scaling the gas transfer velocity and hydraulic geometry in streams and small rivers. *Limnology and Oceanography: Fluids and Environments*, *2*(1), 41–53. https://doi.org/10.1215/21573689-1597669

Regnier, P., Friedlingstein, P., Ciais, P., Mackenzie, F. T., Gruber, N., Janssens, I. A., et al. (2013). Anthropogenic perturbation of the carbon fluxes from land to ocean. *Nature Geoscience*, *6*(8), 597–607. https://doi.org/10.1038/ngeo1830

Regnier, P., Resplandy, L., Najjar, R. G., & Ciais, P. (2022). The land-to-ocean loops of the global carbon cycle. *Nature*, *603*(7901), 401–410. https://doi.org/10.1038/s41586-021-04339-9

Resplandy, L., Keeling, R. F., Eddebbar, Y., Brooks, M., Wang, R., Bopp, L., et al. (2018). Quantification of ocean heat uptake from changes in atmospheric O_2 and CO_2 composition. *Nature*, *563*(7729), 105–108. https://doi.org/10.1038/s41586-018-0651-8

Richey, J. E. (2004). In C. B. Field & M. R. Raupach (Eds.). *The global carbon cycle, integrating humans, climate, and the natural world* (Vol. 17, pp. 329–340). Island Press.

Richey, J. E., Melack, J. M., Aufdenkampe, A. K., Ballester, V. M., & Hess, L. L. (2002). Outgassing from Amazonian rivers and wetlands as a large tropical source of atmospheric CO_2. *Nature*, *416*(6881), 617–620. https://doi.org/10.1038/416617a

Robertson, D. M., & Saad, D. A. (2013). SPARROW models used to understand nutrient sources in the Mississippi/Atchafalaya River Basin. *Journal of Environmental Quality*, *42*(5), 1422–1440. https://doi.org/10.2134/jeq2013.02.0066

Saccardi, B., & Winnick, M. (2021). Improving predictions of stream CO_2 concentrations and fluxes using a stream network model: A case study in the East River watershed, CO, USA. *Global Biogeochemical Cycles*, *35*(12), e2021GB006972. https://doi.org/10.1029/2021gb006972

Scharf, P. C., Wiebold, W. J., & Lory, J. A. (2002). Corn yield response to nitrogen fertilizer timing and deficiency level. *Agronomy Journal*, *94*(3), 435–441. https://doi.org/10.2134/agronj2002.0435

Schlesinger, W. H., & Melack, J. M. (1981). Transport of organic carbon in the world's rivers. *Tellus*, *33*(2), 172–187. https://doi.org/10.3402/tellusa.v33i2.10706

Seitzinger, S. P., Harrison, J., Dumont, E., Beusen, A. H., & Bouwman, A. (2005). Sources and delivery of carbon, nitrogen, and phosphorus to the coastal zone: An overview of Global Nutrient Export from Watersheds (NEWS) models and their application. *Global Biogeochemical Cycles*, *19*(4), GB4S01. https://doi.org/10.1029/2005gb002606

Seitzinger, S. P., Kroeze, C., & Styles, R. V. (2000). Global distribution of N_2O emissions from aquatic systems: Natural emissions and anthropogenic effects. *Chemosphere-Global Change Science*, *2*(3–4), 267–279. https://doi.org/10.1016/s1465-9972(00)00015-5

Stets, E., Kelly, V., & Crawford, C. (2014). Long-term trends in alkalinity in large rivers of the conterminous US in relation to acidification, agriculture, and hydrologic modification. *Science of the Total Environment*, *488*, 280–289. https://doi.org/10.1016/j.scitotenv.2014.04.054

St. Louis, V. L., Kelly, C. A., Duchemin, É., Rudd, J. W. M., & Rosenberg, D. M. (2000). Reservoir surfaces as sources of greenhouse gases to the atmosphere: A global estimate. *BioScience*, *50*(9), 766. https://doi.org/10.1641/0006-3568(2000)050[0766:Rsasog]2.0.Co;2

Tan, Z., Zhuang, Q., & Walter Anthony, K. (2015). Modeling methane emissions from arctic lakes: Model development and site-level study. *Journal of Advances in Modeling Earth Systems*, *7*(2), 459–483. https://doi.org/10.1002/2014MS000344

Thomann, R. V., & Mueller, J. A. (1987). *Principles of surface water quality modeling and control*. Harper & Row Publishers.

Thornton, P. E., & Rosenbloom, N. A. (2005). Ecosystem model spin-up: Estimating steady state conditions in a coupled terrestrial carbon and nitrogen cycle model. *Ecological Modelling*, *189*(1–2), 25–48. https://doi.org/10.1016/j.ecolmodel.2005.04.008

Tian, H., Chen, G., Liu, M., Zhang, C., Sun, G., Lu, C., et al. (2010). Model estimates of net primary productivity, evapotranspiration, and water use efficiency in the terrestrial ecosystems of the southern United States during 1895–2007. *Forest Ecology and Management*, *259*(7), 1311–1327. https://doi.org/10.1016/j.foreco.2009.10.009

Tian, H., Chen, G., Zhang, C., Liu, M., Sun, G., Chappelka, A., et al. (2012). Century-scale responses of ecosystem carbon storage and flux to multiple environmental changes in the southern United States. *Ecosystems*, *15*(4), 674–694. https://doi.org/10.1007/s10021-012-9539-x

Tian, H., Ren, W., Yang, J., Tao, B., Cai, W. J., Lohrenz, S. E., et al. (2015a). Climate extremes dominating seasonal and interannual variations in carbon export from the Mississippi River Basin. *Global Biogeochemical Cycles*, *29*(9), 1333–1347. https://doi.org/10.1002/2014gb005068

Tian, H., Yang, J., Lu, C., Xu, R., Canadell, J. G., Jackson, R. B., et al. (2018). The global N_2O model intercomparison project. *Bulletin of the American Meteorological Society*, *99*(6), 1231–1251. https://doi.org/10.1175/bams-d-17-0212.1

Tian, H., Yang, Q., Najjar, R. G., Ren, W., Friedrichs, M. A. M., Hopkinson, C. S., & Pan, S. (2015b). Anthropogenic and climatic influences on carbon fluxes from eastern North America to the Atlantic ocean: A process-based modeling study. *Journal of Geophysical Research: Biogeosciences*, *120*(4), 757–772. https://doi.org/10.1002/2014jg002760

Viovy, N. (2018). *CRUNCEP version 7-atmospheric forcing data for the community land model* (Vol. 10). Research Data Archive at the National Center for Atmospheric Research, Computational and Information Systems Laboratory.

Vitousek, P. M., & Howarth, R. W. (1991). Nitrogen limitation on land and in the sea: How can it occur? *Biogeochemistry*, *13*(2), 87–115. https://doi.org/10.1007/bf00002772

Williams, J., & Berndt, H. (1977). Sediment yield prediction based on watershed hydrology. *Transactions of the ASAE*, *20*(6), 1100–1104. https://doi.org/10.13031/2013.35710

Wollheim, W. M., Vörösmarty, C. J., Bouwman, A., Green, P., Harrison, J., Linder, E., et al. (2008). Global N removal by freshwater aquatic systems using a spatially distributed, within-basin approach. *Global Biogeochemical Cycles*, *22*(2), GB2026. https://doi.org/10.1029/2007gb002963

Wu, H., Kimball, J. S., Li, H., Huang, M., Leung, L. R., & Adler, R. F. (2012). A new global river network database for macroscale hydrologic modeling. *Water Resources Research*, *48*(9), W09701. https://doi.org/10.1029/2012wr012313

Yao, Y., Tian, H., Pan, S., Najjar, R. G., Friedrichs, M. A. M., Bian, Z., et al. (2021). Riverine carbon cycling over the past century in the Mid-Atlantic region of the United States. *Journal of Geophysical Research: Biogeosciences*, *126*(5), e2020JG005968. https://doi.org/10.1029/2020jg005968

Yao, Y., Tian, H., Shi, H., Pan, S., Xu, R., Pan, N., & Canadell, J. G. (2020). Increased global nitrous oxide emissions from streams and rivers in the Anthropocene. *Nature Climate Change*, *10*(2), 138–142. https://doi.org/10.1038/s41558-019-0665-8

Yao, Y., Tian, H., Xu, X., Li, Y., & Pan, S. (2022). Dynamics and controls of inland water CH_4 emissions across the conterminous United States: 1860-2019. *Water Research*, *224*, 119043. https://doi.org/10.1016/j.watres.2022.119043

Yvon-Durocher, G., Caffrey, J. M., Cescatti, A., Dossena, M., Giorgio, P. d., Gasol, J. M., et al. (2012). Reconciling the temperature dependence of respiration across timescales and ecosystem types. *Nature*, *487*(7408), 472–476. https://doi.org/10.1038/nature11205

Zhang, B., Tian, H., Lu, C., Dangal, S. R., Yang, J., & Pan, S. (2017). Global manure nitrogen production and application in cropland during 1860–2014: A 5 arcmin gridded global dataset for earth system modeling. *Earth System Science Data*, *9*(2), 667–678. https://doi.org/10.5194/essd-9-667-2017

Zhang, H., Lauerwald, R., Ciais, P., Van Oost, K., Guenet, B., & Regnier, P. (2022). Global changes alter the amount and composition of land carbon deliveries to European rivers and seas. *Communications Earth Environment*, *3*(1), 245. https://doi.org/10.1038/s43247-022-00575-7

Zhang, Z., Craft, C. B., Xue, Z., Tong, S., & Lu, X. (2016). Regulating effects of climate, net primary productivity, and nitrogen on carbon sequestration rates in temperate wetlands, Northeast China. *Ecological Indicators*, *70*, 114–124. https://doi.org/10.1016/j.ecolind.2016.05.041

References From the Supporting Information

Arnhold, S., Lindner, S., Lee, B., Martin, E., Kettering, J., Nguyen, T. T., et al. (2014). Conventional and organic farming: Soil erosion and conservation potential for row crop cultivation. *Geoderma*, *219*, 89–105. https://doi.org/10.1016/j.geoderma.2013.12.023

Bird, M., Robinson, R., Oo, N. W., Aye, M. M., Lu, X., Higgitt, D., et al. (2008). A preliminary estimate of organic carbon transport by the Ayeyarwady (Irrawaddy) and Thanlwin (Salween) Rivers of Myanmar. *Quaternary International*, *186*(1), 113–122. https://doi.org/10.1016/j.quaint.2007.08.003

Carroll, C., Halpin, M., Burger, P., Bell, K., Sallaway, M., & Yule, D. (1997). The effect of crop type, crop rotation, and tillage practice on runoff and soil loss on a Vertisol in central Queensland. *Soil Research*, *35*(4), 925–940. https://doi.org/10.1071/s96017

Chang, R., Li, N., Sun, X., Hu, Z., Bai, X., & Wang, G. (2018). Nitrogen addition reduces dissolved organic carbon leaching in a montane forest. *Soil Biology and Biochemistry*, *127*, 31–38. https://doi.org/10.1016/j.soilbio.2018.09.006

Don, A., & Schulze, E.-D. (2008). Controls on fluxes and export of dissolved organic carbon in grasslands with contrasting soil types. *Biogeochemistry*, *91*(2), 117–131. https://doi.org/10.1007/s10533-008-9263-y

Douglas, C., Jr., King, K., & Zuzel, J. (1998). Nitrogen and phosphorus in surface runoff and sediment from a wheat-pea rotation in northeastern Oregon (0047-2425).

Erskine, W. D., Mahmoudzadeh, A., & Myers, C. (2002). Land use effects on sediment yields and soil loss rates in small basins of Triassic sandstone near Sydney, NSW, Australia. *Catena*, *49*(4), 271–287. https://doi.org/10.1016/s0341-8162(02)00065-6

Fang, Y., Zhu, W., Gundersen, P., Mo, J., Zhou, G., & Yoh, M. (2009). Large loss of dissolved organic nitrogen from nitrogen-saturated forests in subtropical China. *Ecosystems*, *12*(1), 33–45. https://doi.org/10.1007/s10021-008-9203-7

Fleming, N., & Cox, J. (2001). Carbon and phosphorus losses from dairy pasture in South Australia. *Soil Research*, *39*(5), 969–978. https://doi.org/10.1071/sr00042

Fröberg, M., Kleja, D. B., Bergkvist, B., Tipping, E., & Mulder, J. (2005). Dissolved organic carbon leaching from a coniferous forest floor--a field manipulation experiment. *Biogeochemistry*, *75*(2), 271–287. https://doi.org/10.1007/s10533-004-7585-y

Ghidey, F., & Alberts, E. (1998). Runoff and soil losses as affected by corn and soybean tillage systems. *Journal of Soil Water Conservation*, *53*(1), 64–70.

Hafner, S. D., Groffman, P. M., & Mitchell, M. J. (2005). Leaching of dissolved organic carbon, dissolved organic nitrogen, and other solutes from coarse woody debris and litter in a mixed forest in New York State. *Biogeochemistry*, *74*(2), 257–282. https://doi.org/10.1007/s10533-004-4722-6

Herbrich, M., Gerke, H. H., Bens, O., & Sommer, M. (2017). Water balance and leaching of dissolved organic and inorganic carbon of eroded Luvisols using high precision weighing lysimeters. *Soil and Tillage Research*, *165*, 144–160. https://doi.org/10.1016/j.still.2016.08.003

Hollinger, E., Cornish, P. S., Baginska, B., Mann, R., & Kuczera, G. (2001). Farm-scale stormwater losses of sediment and nutrients from a market garden near Sydney, Australia. *Agricultural Water Management*, *47*(3), 227–241. https://doi.org/10.1016/s0378-3774(00)00107-4

Hulugalle, N., Rohde, K., & Yule, D. (2002). Cropping systems and bed width effects on runoff, erosion and soil properties in a rainfed Vertisol. *Land Degradation & Development*, *13*(5), 363–374. https://doi.org/10.1002/ldr.510

Hussain, M. Z., Robertson, G. P., Basso, B., & Hamilton, S. K. (2020). Leaching losses of dissolved organic carbon and nitrogen from agricultural soils in the upper US Midwest. *Science of the Total Environment*, *734*, 139379. https://doi.org/10.1016/j.scitotenv.2020.139379

Jacinthe, P.-A., Lal, R., Owens, L., & Hothem, D. (2004). Transport of labile carbon in runoff as affected by land use and rainfall characteristics. *Soil and Tillage Research*, *77*(2), 111–123. https://doi.org/10.1016/j.still.2003.11.004

Juutinen, S., Väliranta, M., Kuutti, V., Laine, A., Virtanen, T., Seppä, H., et al. (2013). Short-term and long-term carbon dynamics in a northern peatland-stream-lake continuum: A catchment approach. *Journal of Geophysical Research: Biogeosciences*, *118*(1), 171–183. https://doi.org/10.1002/jgrg.20028

Koprivnjak, J.-F., & Moore, T. (1992). Sources, sinks, and fluxes of dissolved organic carbon in subarctic fen catchments. *Arctic Alpine Research*, *24*(3), 204–210. https://doi.org/10.2307/1551658

Koskinen, M., Sallantaus, T., & Vasander, H. (2011). Post-restoration development of organic carbon and nutrient leaching from two ecohydrologically different peatland sites. *Ecological Engineering*, *37*(7), 1008–1016. https://doi.org/10.1016/j.ecoleng.2010.06.036

Lentz, R. D., & Lehrsch, G. A. (2014). Manure and fertilizer effects on carbon balance and organic and inorganic carbon losses for an irrigated corn field. *Soil Science Society of America Journal*, *78*(3), 987–1002. https://doi.org/10.2136/sssaj2013.07.0261

Long, G.-Q., Jiang, Y.-J., & Sun, B. (2015). Seasonal and inter-annual variation of leaching of dissolved organic carbon and nitrogen under long-term manure application in an acidic clay soil in subtropical China. *Soil and Tillage Research*, *146*, 270–278. https://doi.org/10.1016/j.still.2014.09.020

Lv, Q., Wang, Y., Li, Y., & Tang, L. (2013). Experimental study on carbon leaching during irrigation in arid areas. *Arid Zone Research*, *36*(3), 450–456.

McDowell, W. H., & Likens, G. E. (1988). Origin, composition, and flux of dissolved organic carbon in the Hubbard Brook Valley. *Ecological Monographs*, *58*(3), 177–195. https://doi.org/10.2307/2937024

McTiernan, K. B., Jarvis, S., Scholefield, D., & Hayes, M. (2001). Dissolved organic carbon losses from grazed grasslands under different management regimes. *Water Research*, *35*(10), 2565–2569. https://doi.org/10.1016/s0043-1354(00)00528-5

Moore, T. (1988). Dissolved iron and organic matter in northern peatlands. *Soil Science*, *145*(1), 70–76. https://doi.org/10.1097/00010694-198801000-00010

Nakatsuka, T., Toda, M., Kawamura, K., & Wakatsuchi, M. (2004). Dissolved and particulate organic carbon in the Sea of Okhotsk: Transport from continental shelf to ocean interior. *Journal of Geophysical Research*, *109*(C9), C09S14. https://doi.org/10.1029/2003jc001909

Ngatunga, E., Lal, R., & Uriyo, A. (1984). Effects of surface management on runoff and soil erosion from some plots at Mlingano, Tanzania. *Geoderma*, *33*(1), 1–12. https://doi.org/10.1016/0016-7061(84)90086-7

Ni, H.-G., Lu, F.-H., Luo, X.-L., Tian, H.-Y., & Zeng, E. Y. (2008). Riverine inputs of total organic carbon and suspended particulate matter from the Pearl River Delta to the coastal ocean off South China. *Marine Pollution Bulletin*, *56*(6), 1150–1157. https://doi.org/10.1016/j.marpolbul.2008.02.030

Olefeldt, D., & Roulet, N. T. (2014). Permafrost conditions in peatlands regulate magnitude, timing, and chemical composition of catchment dissolved organic carbon export. *Global Change Biology*, *20*(10), 3122–3136. https://doi.org/10.1111/gcb.12607

Owens, L., Malone, R., Hothem, D., Starr, G., & Lal, R. (2002). Sediment carbon concentration and transport from small watersheds under various conservation tillage practices. *Soil and Tillage Research*, *67*(1), 65–73. https://doi.org/10.1016/s0167-1987(02)00031-4

Prasuhn, V. (2012). On-farm effects of tillage and crops on soil erosion measured over 10 years in Switzerland. *Soil and Tillage Research*, *120*, 137–146. https://doi.org/10.1016/j.still.2012.01.002

Prokushkin, A., Pokrovsky, O., Shirokova, L., Korets, M., Viers, J., Prokushkin, S., et al. (2011). Sources and the flux pattern of dissolved carbon in rivers of the Yenisey basin draining the Central Siberian Plateau. *Environmental Research Letters*, *6*(4), 045212. https://doi.org/10.1088/1748-9326/6/4/045212

Ramos, M., & Martínez-Casasnovas, J. (2006). Nutrient losses by runoff in vineyards of the Mediterranean Alt Penedès region (NE Spain). *Agriculture, Ecosystems & Environment*, *113*(1–4), 356–363. https://doi.org/10.1016/j.agee.2005.10.009

Rice, P. J., McConnell, L. L., Heighton, L. P., Sadeghi, A. M., Isensee, A. R., Teasdale, J. R., et al. (2001). Runoff loss of pesticides and soil: A comparison between vegetative mulch and plastic mulch in vegetable production systems. *Journal of Environmental Quality*, *30*(5), 1808–1821. https://doi.org/10.2134/jeq2001.3051808x

Rieckh, H., Gerke, H. H., Sommer, M., & Siemens, J. (2013). Vertical water and DOC/DIC flux estimates in a hummocky groundmoraine soil landscape. In *Paper presented at the EGU general assembly conference abstracts*.

Said-Pullicino, D., Miniotti, E. F., Sodano, M., Bertora, C., Lerda, C., Chiaradia, E. A., et al. (2016). Linking dissolved organic carbon cycling to organic carbon fluxes in rice paddies under different water management practices. *Plant and Soil*, *401*(1), 273–290. https://doi.org/10.1007/s11104-015-2751-7

Schindlbacher, A., Beck, K., Holzheu, S., & Borken, W. (2019). Inorganic carbon leaching from a warmed and irrigated carbonate forest soil. *Frontiers in Forests Global Change*, *2*, 40. https://doi.org/10.3389/ffgc.2019.00040

Soileau, J., Touchton, J., Hajek, B., & Yoo, K. (1994). Sediment, nitrogen, and phosphorus runoff with conventional-and conservation-tillage cotton in a small watershed. *Journal of Soil Water Conservation*, *49*(1), 82–89.

Strohmeier, S., Knorr, K.-H., Reichert, M., Frei, S., Fleckenstein, J., Peiffer, S., & Matzner, E. (2013). Concentrations and fluxes of dissolved organic carbon in runoff from a forested catchment: Insights from high frequency measurements. *Biogeosciences*, *10*(2), 905–916. https://doi.org/10.5194/bg-10-905-2013

Urban, N., Bayley, S., & Eisenreich, S. (1989). Export of dissolved organic carbon and acidity from peatlands. *Water Resources Research*, *25*(7), 1619–1628. https://doi.org/10.1029/wr025i007p01619

Versini, A., Mareschal, L., Matsoumbou, T., Zeller, B., Ranger, J., & Laclau, J.-P. (2014). Effects of litter manipulation in a tropical Eucalyptus plantation on leaching of mineral nutrients, dissolved organic nitrogen and dissolved organic carbon. *Geoderma*, *232*, 426–436. https://doi.org/10.1016/j.geoderma.2014.05.018

Villatoro-Sánchez, M., Le Bissonnais, Y., Moussa, R., & Rapidel, B. (2015). Temporal dynamics of runoff and soil loss on a plot scale under a coffee plantation on steep soil (Ultisol), Costa Rica. *Journal of Hydrology*, *523*, 409–426. https://doi.org/10.1016/j.jhydrol.2015.01.058

Walmsley, D. C., Siemens, J., Kindler, R., Kirwan, L., Kaiser, K., Saunders, M., et al. (2011). Dissolved carbon leaching from an Irish cropland soil is increased by reduced tillage and cover cropping. *Agriculture, Ecosystems & Environment*, *142*(3–4), 393–402. https://doi.org/10.1016/j.agee.2011.06.011

Wang, X., Ma, H., Li, R., Song, Z., & Wu, J. (2012). Seasonal fluxes and source variation of organic carbon transported by two major Chinese Rivers: The Yellow River and Changjiang (Yangtze) River. *Global Biogeochemical Cycles*, *26*(2), GB2025. https://doi.org/10.1029/2011gb004130

Wang, Z. A., Bienvenu, D. J., Mann, P. J., Hoering, K. A., Poulsen, J. R., Spencer, R. G., & Holmes, R. M. (2013). Inorganic carbon speciation and fluxes in the Congo River. *Geophysical Research Letters*, *40*(3), 511–516. https://doi.org/10.1002/grl.50160

Wit, F., Müller, D., Baum, A., Warneke, T., Pranowo, W. S., Müller, M., & Rixen, T. (2015). The impact of disturbed peatlands on river outgassing in Southeast Asia. *Nature Communications*, *6*(1), 1–9. https://doi.org/10.1038/ncomms10155

You, Y., Xiang, W., Ouyang, S., Zhao, Z., Chen, L., Zeng, Y., et al. (2020). Hydrological fluxes of dissolved organic carbon and total dissolved nitrogen in subtropical forests at three restoration stages in southern China. *Journal of Hydrology*, *583*, 124656. https://doi.org/10.1016/j.jhydrol.2020.124656